Carderock Division, Naval Surface Warfare Center
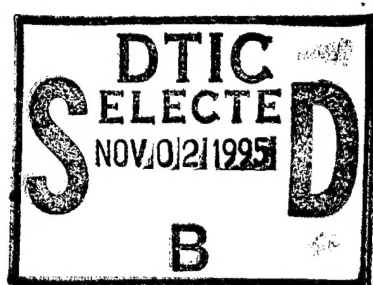
Bethesda, Md 20084-5000

Predicting the Motions of SWATH Ships in Waves - A Validated Mathematical Model

by
Kathryn K. McCreight

DTIC
ELECTE
NOV 02 1995
B

19951031 121

DTIC QUALITY INSPECTED 3

MAJOR CARDEROCK DIVISION TECHNICAL COMPONENTS

CODE 011 Director of Technology

10 Machinery Systems/Programs and Logistics Directorate

20 Ship Systems & Programs Directorate

50 Hydromechanics Directorate

60 Survivability, Structures and Materials Directorate

70 Signatures Directorate

80 Machinery Research & Development Directorate

90 Machinery In-Service Engineering Directorate

CARDEROCK DIVISION, NSWC, ISSUES THREE TYPES OF REPORTS:

1. **CARDEROCKDIV reports, a formal series,** contain information of permanent technical value. They carry a consecutive numerical identification regardless of their classification or the originating directorate.

2. **Directorate reports, a semiformal series,** contain information of a preliminary, temporary, or proprietary nature or of limited interest or significance. They carry an alphanumerical identification issued by the originating directorate.

3. **Technical memoranda, an informal series,** contain technical documentation of limited use and interest. They are primarily working papers intended for internal use. They carry an identifying number which indicates their type and the numerical code of the originating directorate. Any distribution outside CARDEROCKDIV must be approved by the head of the originating directorate on a case-by-case basis.

REPORT DOCUMENTATION PAGE

1a. REPORT SECURITY CLASSIFICATION	1b. RESTRICTIVE MARKINGS
Unclassified	

2a. SECURITY CLASSIFICATION AUTHORITY	3. DISTRIBUTION / AVAILABILITY OF REPORT
	Approved for public release. Distribution unlimited.
2b. DECLASSIFICATION / DOWNGRADING SCHEDULE	

4. PERFORMING ORGANIZATION REPORT NUMBER(S)	5. MONITORING ORGANIZATION REPORT NUMBER(S)
CRDKNSWC / SHD-1350-03	

6a. NAME OF PERFORMING ORGANIZATION	6b. OFFICE SYMBOL *(If applicable)*	7a. NAME OF MONITORING ORGANIZATION
Naval Surface Warfare Center, Carderock Division	562	Naval Sea Systems Command

6c. ADDRESS *(City, State, and Zip Code)*	7b. ADDRESS *(City, State, and Zip Code)*
Bethesda, MD 20084-5000	Washington, D.C. 20362

8a. NAME OF FUNDING / SPONSORING ORGANIZATION	8b. OFFICE SYMBOL *(If applicable)*	9. PROCUREMENT INSTRUMENT IDENTIFICATION NUMBER
Naval Sea Systems Command	SEA 03H	

8c. ADDRESS *(City, State, and Zip Code)*	10. SOURCE OF FUNDING NUMBERS			
	PROGRAM ELEMENT NO.	PROJECT NO.	TASK NO.	WORK UNIT ACCESSION NO.
Washington, D.C. 20362	64567N		AA10357	1-1237-326

11. TITLE *(Include Security Classification)*
Predicting the Motions of SWATH Ships - A Validated Mathematical Model

12. PERSONAL AUTHOR(S)
Kathryn K. McCreight

13a. TYPE OF REPORT	13b. TIME COVERED	14. DATE OF REPORT *(Year, Month, Day)*	15. PAGE COUNT
Final	FROM_____ TO_____	1995 June	63

16. SUPPLEMENTARY NOTATION

17.	COSATI CODES		18. SUBJECT TERMS *(Continue on reverse if necessary and identify by block number)*
FIELD	GROUP	SUB-GROUP	SWATH motions, seakeeping, motion prediction

19. ABSTRACT *(Continue on reverse if necessary and identify by block number)*

A mathematical model for predicting the motions of SWATH ships in waves in the frequency domain is presented. This mathematical model requires definition of only geometric and mass properties. While the mathematical model for the vertical plane presented here differs little from the one which has been used for about a decade, the transverse plane model differs from the previous model in various ways. Predictions are compared to measured model experimental responses to regular waves. These results show that the responses to regular waves are well-predicted for a range of hull forms and conditions.

DTIC QUALITY INSPECTED 3

20. DISTRIBUTION / AVAILABILITY OF ABSTRACT	21. ABSTRACT SECURITY CLASSIFICATION	
☐ UNCLASSIFIED/UNLIMITED ☒ SAME AS RPT ☐ DTIC USERS	Unclassified	

22a. NAME OF RESPONSIBLE INDIVIDUAL	22b. TELEPHONE *(Include Area Code)*	22c. OFFICE SYMBOL
Kathryn K. McCreight	(301) 227-1242	562

DD Form 1473, JUN 86   (Reverse)

ii

CONTENTS

FIGURES

TABLES

NOMENCLATURE

a_{f_i} is the approximate added mass of the ith appendage

a_{jk} is the two-dimensional added mass coefficient in the jth mode due to the kth motion

a_{0H} is the lift coefficient in the horizontal plane

a_{0V} is the vertical lift in the vertical plane

A is the wave amplitude

A_{jk} is the added mass coefficient in the jth mode due to the kth motion

$(A_{jk})_A$ is the contribution of the appendages to A_{jk}

$(A_{jk})_{PF}$ is the potential flow contribution to A_{jk}

A_{f_i} is the projected area of the ith appendage

AR_i is the effective aspect ratio of the ith appendage

AR_S is the aspect ratio of a strut

b_i is the span of the ith appendage

b_{jk} is the two-dimensional damping coefficient in the jth mode due to the kth motion

$\overline{BG}$ is the distance between the center of buoyancy and the center of gravity

B_{jk} is the damping coefficient in the jth mode due to the kth motion

$(B_{jk})_A$ is the contribution of the appendages to B_{jk}

$(B_{jk})_{BL+CD}$ is the body lift and cross flow drag contributions to B_{jk}

$(B_{jk})_{PF}$ is the potential flow ontribution to B_{jk}

c_i is the mean chord of the ith appendage

C_{D_F} is the cross flow drag coefficient for the ith appendage

C_{DH} is the cross flow drag coefficient for the horizontal plane

C_{DH_P} and C_{DH_S} are the cross flow drag coefficients for the horizontal plane for the port and starboard hulls

C_{jk} is the restoring coefficient in the jth mode due to the kth motion

$(C_{jk})_A$ is the contribution of the appendages to C_{jk}

$(C_{jk})_{BL+CD}$ is the body lift and cross flow drag contributions to C_{jk}

$(C_{jk})_{PF}$ is the potential flow contribution to C_{jk}

$C_{L\alpha_i}$ is the lift curve slope of the ith appendage

C_{Lc} is a modification factor to reflect the effect of downwash from one appendage on another

C_{DV} is the cross flow drag coefficient for the vertical plane

C_{DV_P}, C_{DV_S} are the cross flow drag coefficients for the vertical plane for the port and starboard hulls

D is a diameter

d is the transverse projection of the body

d_1 is the depth to the maximum beam of the hull or half the draft for strut only sections

d_2 is a moment arm defined to be equal to d_1 for fully submerged sections and $d/2$ for other sections

d_H the horizontal diameter of the lower hull

d_V is the vertical diameter of the lower hull

F_H is the horizontal force for a body with a moderate drift angle relative to the flow

F_j is wave exciting force of the ship in the jth mode

$(F_j)_A$ is the contribution of the appendages to F_j

$(F_j)_{BL+CD}$ is the body lift and cross flow drag contributions to F_j

$(F_j)_{PF}$ is the potential flow contribution to F_j

F_V is the vertical force for an inclined body at a moderate angle of incidence relative to the flow

I_4, I_5, I_6 are the mass moments of inertia in roll, pitch, and yaw

k is the wave number

KC is the Keulegan-Carpenter number

L is the length of the ship

m' is the mass of the unappended ship nondimensionalized

m_{f_i} is the approximate mass of the ith appendage

$(m_{jk})_A$ is the contribution of the appendages to the mass matrix

M is the mass of the displaced volume of the ship

n_2 and n_3 are components of the unit vector normal to the body surface

S_D is the distance from the ship centerline to the strut centerline

t is the horizontal thickness of the strut

T is the period of oscillation

U is the forward speed of the ship

v_p, v_s are the relative horizontal velocities for the port and starboard hulls

v_{P_i}, v_{S_i} are the relative horizontal velocities for the ith port and starboard appendages

V_{max} is the amplitude of the relative velocity

w_p, w_s are the relative vertical velocities for the port and starboard hulls

w_{P_i}, w_{S_i} are the relative vertical velocities for the ith port and starboard appendages

x_c is the center of lift of a section of the body

z_{CG} is the z coordinate of the ship's center of gravity

α_i is the cant angle of the appendage relative to the horizon

β is the heading of the ship relative to the wave with $\beta = 180$ for head seas

β_{KC} is a frequency parameter

$\dot{\zeta}_H$ is the horizontal velocity of the fluid induced by the incoming wave

$\dot{\zeta}_V$ is the vertical velocity of the fluid induced by the incoming wave

Λ_i be the sweep angle of the quarter chord line of the ith appendage

ν is the kinematic viscosity of the fluid

ξ_j is the complex displacement of the ship in the jth mode

ρ is the mass density of the fluid

ϕ_0 the complex velocity potential for the incident wave

ϕ_k is the complex velocity potential for forced oscillation in the kth mode

ω is the wave frequency

ω_e is the wave frequency of encounter

ABSTRACT

A mathematical model for predicting the motions of SWATH ships in waves in the frequency domain is presented. This mathematical model requires definition of only geometric and mass properties. While the mathematical model for the vertical plane presented here differs little from the one which has been used for about a decade, the transverse plane model differs from the previous model in various ways. Predictions are compared to measured model experimental responses to regular waves. These results show that the responses to regular waves are well-predicted for a range of hull forms and conditions.

ADMINISTRATIVE INFORMATION

INTRODUCTION

A mathematical model for the motions of a SWATH ship in waves has been developed over a period of years. As described in reference 1, the mathematical model used for SWATH responses to waves follows the strip theory of Salvesen, Tuck, and Faltinsen[2]. Lee[3] applied this theory to twin hull configurations and utilized an expression presented by Thwaites[4] to develop a model for the cross flow drag and body lift contributions to the forces. Hong[5] introduced surge into the model. Subsequently, McCreight and Stahl[6] developed semi-empirical expressions for the cross flow drag and lift contributions for the vertical plane responses and added the effect of downwash on the lift of the aft stabilizers. Accurate modeling of the vertical plane motions was the focus of this last effort; no changes to Lee's[3] mathematical model for the transverse plane motions were made. Recently, the mathematical model for transverse plane motions and the appendages has been modified. Damping terms now couple heave, pitch, and roll.

In this report, the six degrees of freedom mathematical model for the motions of SWATH ships in waves which is implemented in SWMP94 (SWATH Motions Program, 1994 Version) is described. With this model, only geometric and mass properties are required in order to predict the six degrees-of-freedom motions of SWATH ships. Comparisons between model scale experimental results and predictions are presented for vertical and transverse plane motions for various hull forms.

BACKGROUND

Whereas Lee[3] and Hong[5] use the Frank Close Fit Technique[7] to evaluate the velocity potentials, the computer software described and utilized by McCreight[1] and McCreight and Stahl[6] includes approximations. Velocity potentials are not evaluated. Instead, added mass and damping coefficients are approximated using

expressions developed and reported by John Dalzell[*]. Then, with various assumptions and approximations, the wave exciting forces and moments are approximated as a function of added mass and damping. A derivation for approximate heave and pitch exciting forces is given in reference 6, but the derivation for the transverse plane forces which has been in use is not available.

The approximate approach for the added mass and damping coefficients of SWATH configurations was developed by Dalzell in the late 1970's. This approach was advantageous because it significantly reduced computer time (and cost) compared to Frank Close Fit Technique calculations. Consequently, it facilitated evaluation of numerous hull forms in design studies. The approximations assumed that the cross sections had wall-sided struts centered over hulls with elliptical cross sections; this corresponded to the configurations of interest at that time. Subsequent advances in computers diminished the motivation for approximations and a wider variety of cross sections was considered as the SWATH concept matured. Consequently, the Frank Close Fit Technique[7] was incorporated in the U.S. Navy code and was optionally utilized to calculate the added mass and damping coefficients. However, since utilization of the velocity potentials for the exciting forces and moments required a reorganization of the program, the wave exciting forces and moments continued to be calculated as functions of the added mass and damping coefficients.

The computer program which implemented this model is known as the SWATH Motions Program (SWMP). Predictions from SWMP for the vertical plane agreed well with model scale experimental results for all headings through moderate speeds, but predictions for the transverse plane responses were not reliable. Fortunately, for many SWATH configurations, the roll natural period is in a range where little wave energy occurs, resulting in little roll response. However, the need for a more accurate predictions for the transverse plane was clear.

SWMP94, a recent modification of SWMP, implements the mathematical model which is described in this report. In SWMP94, exciting forces and moments are a function of velocity potentials which are calculated using the Frank Close Fit Technique. The mathematical model for the effects of appendages differs somewhat from the one in SWMP. Expressions to define the lift and drag coefficients for the transverse plane are developed. These coefficients vary with the geometry of the ship and are determined within the program. Corrections are made to Lee's[3] derivation for the cross flow drag and lift components for the transverse plane. Also, some of Lee's simplifications are removed. Consequently, the vertical velocities in the cross flow drag contributions to the forces, as well as new damping terms, couple the transverse and vertical planes of motion.

MATHEMATICAL MODEL

In modeling the motions of SWATH ships in waves, a right-handed coordinate system which has x positive forward, z positive up is used. Responses are calculated about the longitudinal center of gravity of the ship at the ship's centerline at the mean calm waterline. The standard linear equations of motion for a rigid body with harmonic

---

[*] Presented by Dalzell in Stevens Institute of Technology reports of limited distribution.

exciting forces are:

$$(M+A_{22})\ddot{\xi}_2 + B_{22}\dot{\xi}_2 + (A_{24} - Mz_{CG})\ddot{\xi}_4 + B_{24}\dot{\xi}_4 + A_{26}\ddot{\xi}_6 + B_{26}\dot{\xi}_6 = F_2 e^{-i\omega_e t}$$

$$(M+A_{33})\ddot{\xi}_3 + B_{33}\dot{\xi}_3 + C_{33}\xi_3 + A_{35}\ddot{\xi}_5 + B_{35}\dot{\xi}_5 + C_{35}\xi_5 = F_3 e^{-i\omega_e t}$$

$$(I_4+A_{44})\ddot{\xi}_4 + B_{44}\dot{\xi}_4 + C_{44}\xi_4 + (A_{42} - Mz_{CG})\ddot{\xi}_2 + B_{42}\dot{\xi}_2 + A_{46}\ddot{\xi}_6 + B_{46}\dot{\xi}_6 = F_4 e^{-i\omega_e t}$$

$$(I_5+A_{55})\ddot{\xi}_5 + B_{55}\dot{\xi}_5 + C_{55}\xi_5 + A_{53}\ddot{\xi}_3 + B_{53}\dot{\xi}_3 + C_{53}\xi_3 = F_5 e^{-i\omega_e t}$$

$$(I_6+A_{66})\ddot{\xi}_6 + B_{66}\dot{\xi}_6 + A_{62}\ddot{\xi}_2 + B_{62}\dot{\xi}_2 + A_{64}\ddot{\xi}_4 + B_{64}\dot{\xi}_4 = F_6 e^{-i\omega_e t}$$

where M is the mass of the displaced volume of the ship; I_4, I_5, I_6 are the mass moments of inertia in roll, pitch, and yaw; z_{CG} is the z coordinate of the ship's center of gravity; and ω_e is the wave frequency of encounter where

$$\omega_e = \omega - \frac{\omega^2}{g} U \cos\beta$$

ω is the wave frequency, g is the acceleration due to gravity, U is the forward speed of the ship, and β is the heading of the ship relative to the wave, with $\beta = 180°$ for head seas. A_{jk} B_{jk}, and C_{jk} are the added mass, damping, and restoring coefficients in the jth mode due to the kth motion where j or k = 2, 3, 4, 5, and 6 for sway, heave, roll, pitch, and yaw, respectively. F_j and ξ_j are the wave exciting force and displacement of the ship in the jth mode where

$$\xi_j = (\xi_{jr} + i\xi_{jc}) e^{-i\omega_e t}$$

The hydrostatic restoring forces are defined by:

$$C_{33} = \rho g \int t \, dx$$

$$C_{35} = C_{53} = \rho g \int x t \, dx$$

$$C_{44} = \rho g \int y^2 t \, dx - Mg\overline{BG}$$

$$C_{55} = \rho g \int x^2 t \, dx - Mg\overline{BG}$$

where t is the thickness of the strut and $\overline{BG}$ is the distance between the center of buoyancy and the center of gravity.

Surge is approximated by:

$$M\ddot{\xi}_1 = F_1 e^{-i\omega_e t}$$

The coefficients A_{jk}, B_{jk}, and C_{jk} and the forces F_j have contributions due to potential flow, cross flow drag, and lift due to the body and the appendages. That is, in general,

$$D = (D)_{PF} + (D)_{BL+BCD} + (D)_A$$

where D may be A_{jk}, B_{jk}, C_{jk} or F_j,: and PF, BL, BCD, A stand for potential flow, body lift, body cross flow drag, appendage, respectively. The formulations for the various components will be given in this report.

Potential Flow Components

The potential flow added mass and damping coefficients and the wave exciting forces for sway, heave, roll, pitch, and yaw are those presented by Lee[3] which result from application of the strip theory of Salvesen, Tuck, and Faltinsen[2] to SWATH ships. Potential flow terms are given in Appendix A.

3

Body Lift and Cross Flow Drag Components

The mathematical model for the body lift and cross flow drag terms which will be presented here is an extension of the one developed by Lee[3]. Some errors in Lee's derivation of the cross flow drag and lift terms for the transverse plane have been corrected. Also, the derivation presented here differs from Lee's in that the relative vertical velocities include heave, pitch, and roll. Consequently, there is a coupling between the vertical and transverse planes due to the relative vertical velocity terms, resulting in the introduction of the terms B_{34}, B_{43}, B_{45}, and B_{54}.

The basic development for the body lift and cross flow drag components is given in Appendix B. Body lift contributions for the vertical plane were developed in a semi-empirical manner, as summarized in Appendix C. A more direct approach is used for the transverse plane, as given in Appendix D. An approach for evaluating the cross flow drag coefficients is given in Appendix E.

Appendage Cross Flow Drag and Lift Components

Development of fin contributions to the coefficients and forces for stabilizing fins is given in reference 3. This model was used in references 1, 5, and 6. In reference 6, an expression for the lift curve slope of the appendages, including a modification for the downwash from the forward fin on a coplanar aft fin was introduced. In unpublished work, Ernest E. Zarnick and Ralph G. Stahl of the David Taylor Model Basin extended Lee's fin model to the case where the appendages may be canted with respect to the horizon. In the model presented here, these canted effects have been retained. However, the appendage mass contributions have been separated from the added mass terms; forward speed terms which had been included have been removed. Expressions for these components are given in Appendix F.

Total Components

The contributions to the added mass, damping, and restoring coefficients and wave exciting forces as described above are summed and presented in Appendix G.

COMPARISON BETWEEN EXPERIMENTAL AND NUMERICAL PREDICTIONS

In this section, responses to regular waves which were measured during model scale experiments and those which were calculated using the mathematical model described in this report are compared in order to check the validity of the mathematical model. Characteristics of the hullforms for which results are presented are given in Table 1. The hullforms are listed in the order in which they were tested. The hullforms have a variety of characteristics. These hull forms were investigated over a long period of time, reflecting a shift from exploration to fully realized ship designs.

Table 1. Some characteristics of hullforms.

	6A	6B	6C	Stretched SSP	TAGOS-81-design	TAGOS-81-heavy	TAGOS-19	TAGOS-23
Displacement, LT	2900	2900	2900	614	3014	3463	3338	5370
LOA, ft	240.0	240.0	240.0	149.1	244.0	244.0	232.50	279.00
Draft, ft	26.67	26.67	26.67	16.5	22.11	29.20	24.75	26.00
SD, ft	75.0	75.0	75.0	40.0	77.10	77.0	71.00	72.00
A_{WP}, ft	2121.8	2123.0	1908.0	725.49	2151.1	2151.1	2685.5	4354.0
LCB, ft	116.3	115.3	113.9	72.11	122.08	122.2	107.90	129.90
LCF, ft	113.85	111.06	108.10	80.02	122.67	122.7	107.41	130.64
G_{ML}, ft	20.0	38.0	45.0	50.52	26.1	38.2	27.80	49.00
G_{MT}, ft	11.06	10.60	10.94	5.25	8.30	14.1	9.20	8.23
KG, ft	34.0	34.0	34.0	14.11	28.8	25.3	31.50	33.80
KB, ft	10.6	10.6	10.6	7.25	8.37	10.53	10.30	11.18
k_θ, ft	55.91	58.79	58.07	40.7	57.0	58.7	41.36	65.90
k_ϕ, ft	39.60	39.76	38.91	18.4	40.7	41.7	29.0	38.8
Struts/Hull	1	1	2	2	1	1	1	1
Length at WL, ft	172.3	208.0	197.5	139.0	199.48	199.48	190.00	230.00
Strut Setback, ft	27.7	7.1	9.4	7.87	16.47	16.47	16.00	19.00
Horiz/Vert Diam.	1.0	1.0	1.0	1.0	1.8	1.8	1.4	1.25
WL to Hull	11.67	11.67	11.67	5.58	9	16.09	8.75	7
WL to midhull	19.17	19.17	19.17	11.15	15.56	22.64	16.75	16.5

A comparison between the experimental and predicted results are given in Figures 1 to 8. The experimental results for the 6A, 6B, and 6C configurations are presented in Reference 16. The experimental results for the other configurations are presented in David Taylor Model Basin reports of limited distribution.[*] Experiments were run for a range of speeds and headings for the various configurations. Bow and quartering waves were both 45 degrees from beam seas. The order of the experimental results corresponds to the order in which the experiments occurred.

---

[*] The experimental results for the Stretched SSP and the 1981 T-AGOS design were reported by A. Gersten. The results for the T-AGOS 19 were reported by R. Thomas Waters and David D. Hayden and the experimental investigation for the T-AGOS 23 was reported by James W. Hickok, Jr. and Ralph Stahl.

There are differences between the conditions which are assumed in the mathematical model and those which are possible during experiments. In the mathematical development it is assumed that speed and relative wave heading are constant. In the experiments it can be difficult to maintain these conditions, particularly in oblique headings. Models are self-propelled and are tethered to the carriage which moves above the model. Speed and deflection of control surfaces are controlled manually. While application of advances in electronics have made it easier to maintain speed and heading, the dominant factor in control of the model is speed. Since lift is proportional to speed squared, the ability to control a model (or ship) increases significantly with speed.

For some of the configurations, measured roll is presented for head and following waves. In head or following waves, if the waves are purely two-dimensional and the heading is precise, a symmetric ship will have no roll response. Consequently, the magnitude of roll in these conditions gives a measure of the extent to which the intended relative wave heading conditions were not met.

Another difficulty is that under some conditions the model will surge or significantly deviate from its intended course, resulting in taught tethers. This is particularly challenging at zero speed. One innovation which was introduced in the more recent tests is used for beam seas at zero speed. In this case, the model is turned 90° relative to its usual orientation to the carriage, waves are generated from the short bank, and the model is allowed to drift with the waves while the carriage moves with it. This alleviates the interference of the tethers with the model.

SWATH responses have been shown to be nonlinear[16] with respect to wave amplitude, particularly at low speed. The mathematical model presented in this report models this behavior with the introduction of the cross flow drag components and application of equilinearization. When calculations are made, a value for wave amplitude is needed. In comparing predictions with experimental results it is convenient to specify wave slope (the ratio of wave height to wave length). In the predictions which are presented here, two values of wave slope are used in order to bracket the values used in the model experiments. Consequently, there are two curves of predictions on each plot.

CONCLUSIONS

A frequency domain mathematical model for the responses of SWATH ships to regular waves has been presented. The model requires a description of the hullform geometry and mass characteristics. Expressions have been developed for explicitly evaluating the various lift and cross flow drag components. These utilize experimental results from a range of sources. Correlation with model experimental results is excellent for a variety of hull forms, across a range of headings and speeds.

ACKNOWLEDGEMENT

Figure 1 - Comparison of experimental and predicted motion transfer functions
for two different wave slopes for the SWATH 6A.

7

Figure 1 (Continued)

8

Figure 1 (Continued)

9

Figure 1 (Continued)

10

Figure 2 - Comparison of experimental and predicted motion transfer functions for two different wave slopes for the SWATH 6B.

11

Figure 2 (Continued)

Figure 2 (Continued)

13

Figure 2 (Continued)
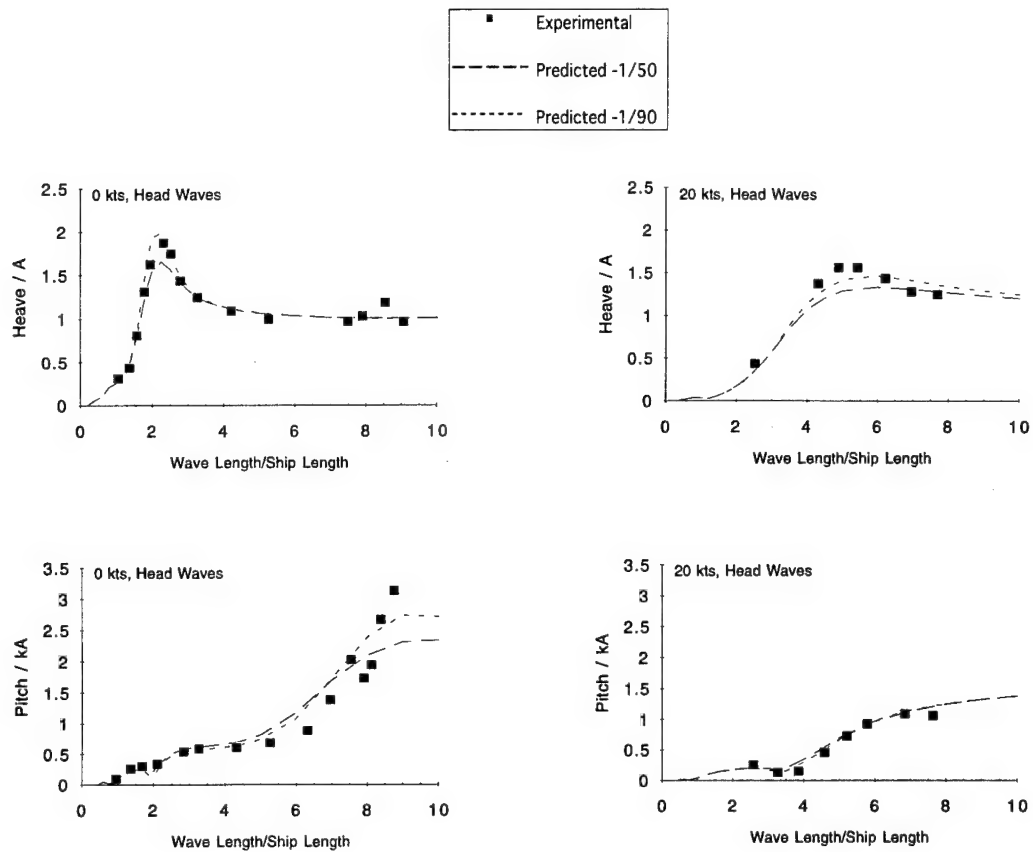
14

Figure 3 - Comparison of Experimental and Predicted Motion Transfer Functions
for two different wave slopes for the SWATH 6C.

15

Figure 3 (Continued)

16

Figure 3 (Continued)

17

Legend:
- ■ Experimental
- Predicted -1/50 (dashed line)
- Predicted -1/90 (dotted line)

20 kts, Following Waves (Heave / A vs Wave Length/Ship Length)

20 kts, Following Waves (Pitch / kA vs Wave Length/Ship Length)

Figure 3 (Continued)

Figure 4 - Comparison of experimental and predicted motion transfer functions
for two different wave slopes for the Stretched SSP.

19

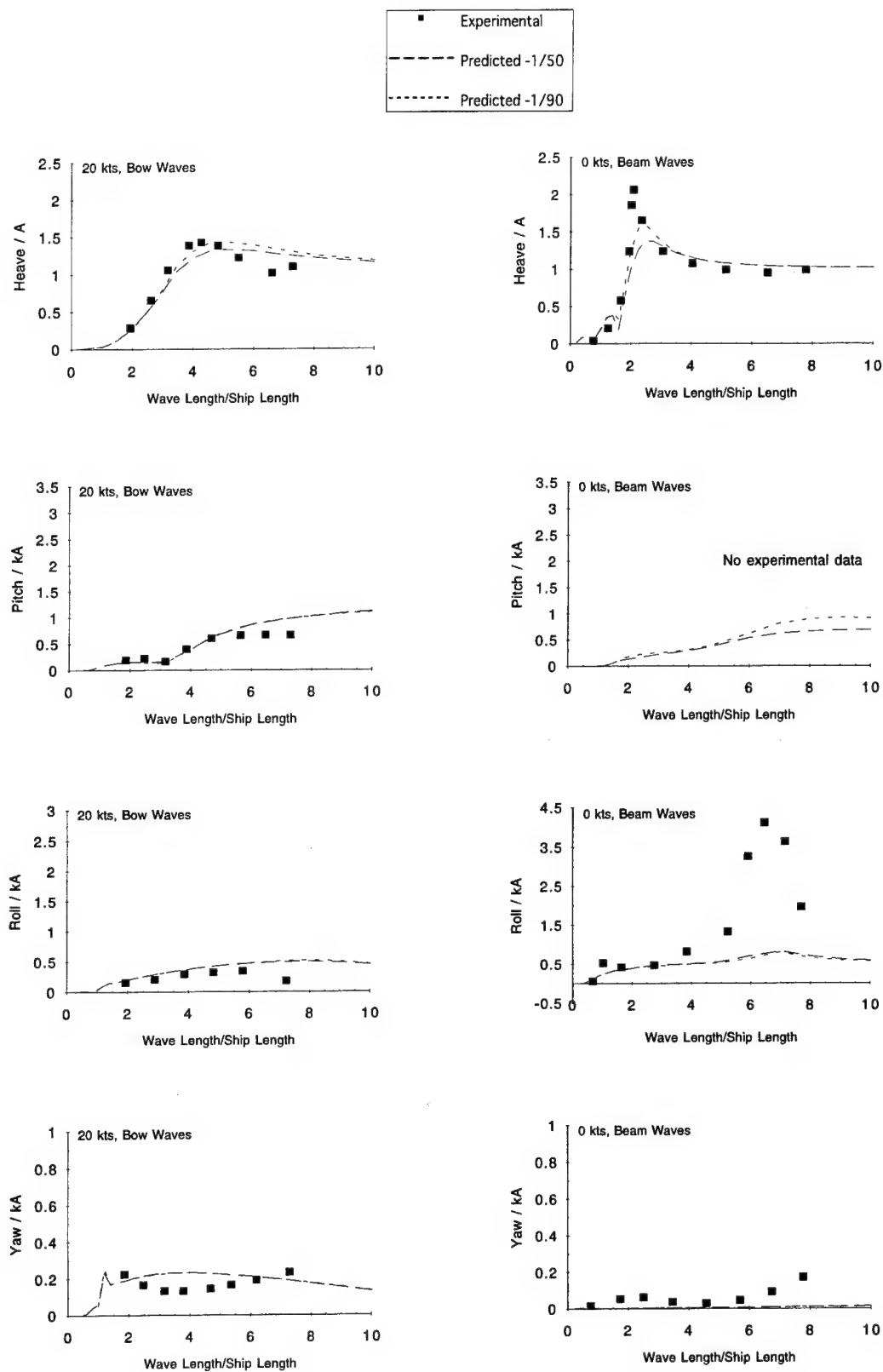Figure 4 (Continued)

20

Figure 4 (Continued)

21
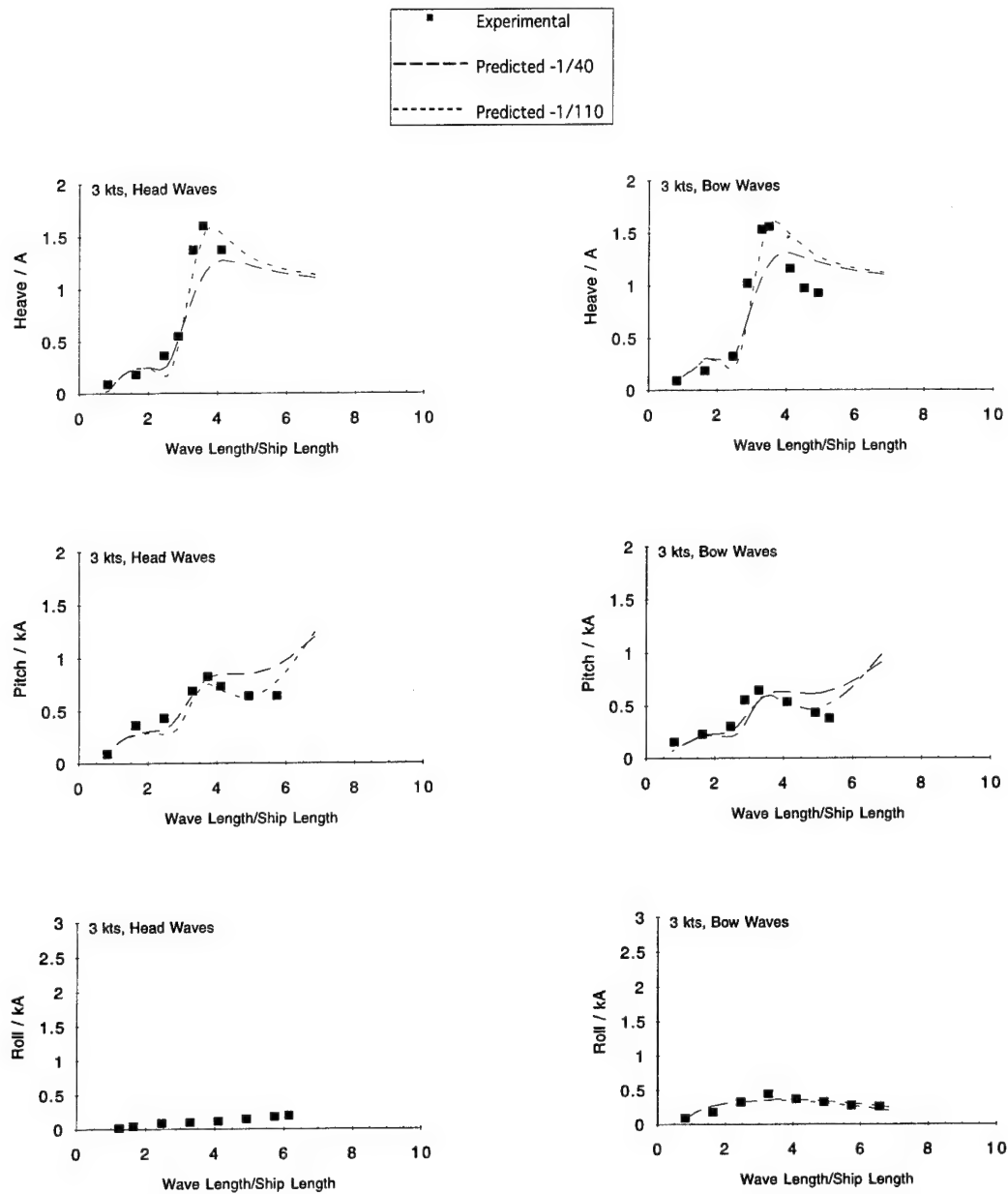
Figure 5 - Comparison of experimental and predicted motion transfer functions
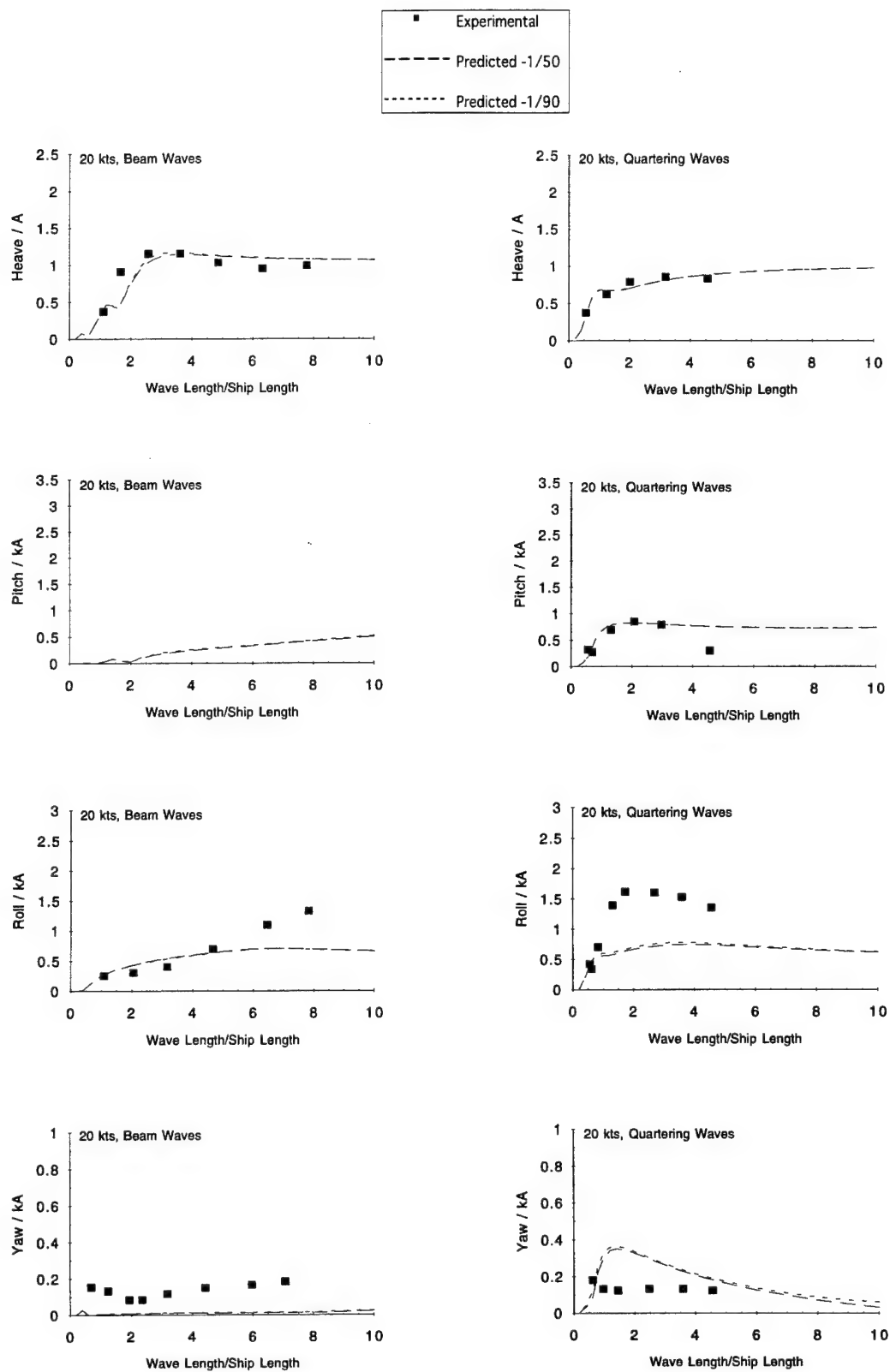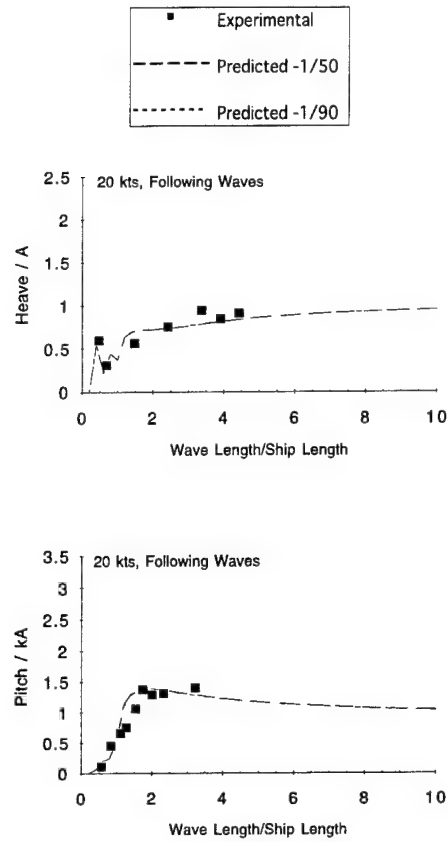for two different wave slopes for the 1981 T-AGOS at the design draft.

Figure 5 (Continued)

23

Figure 5 (Continued)

24
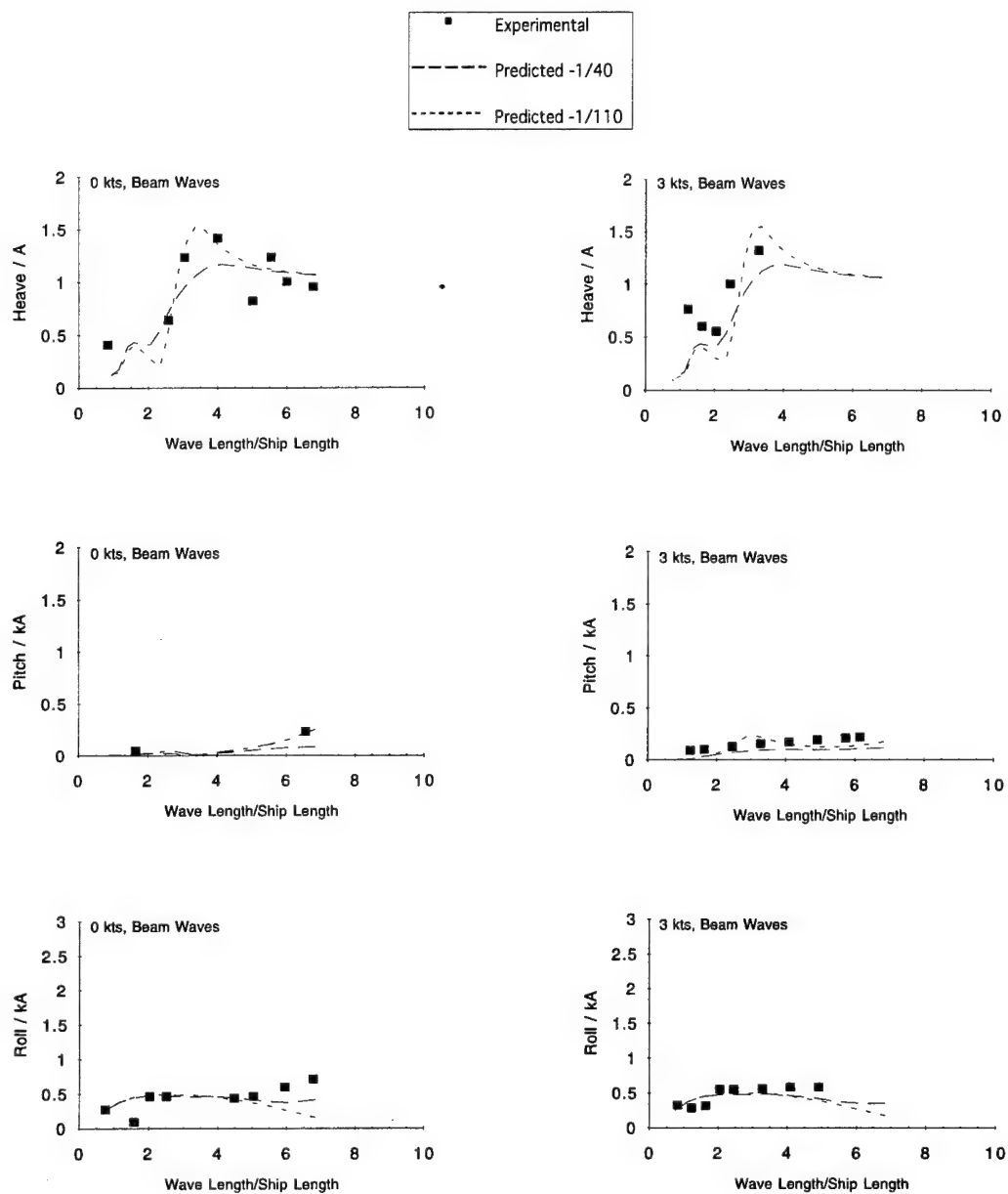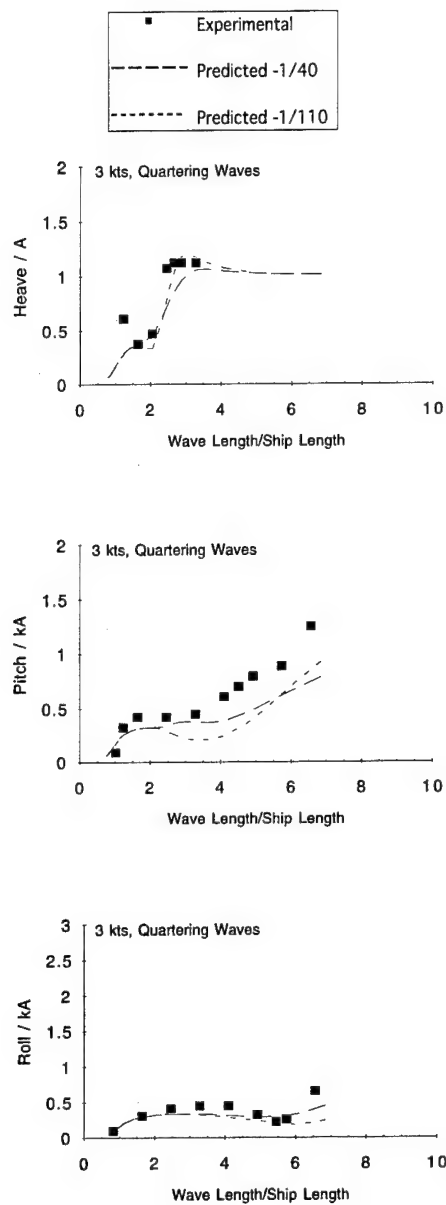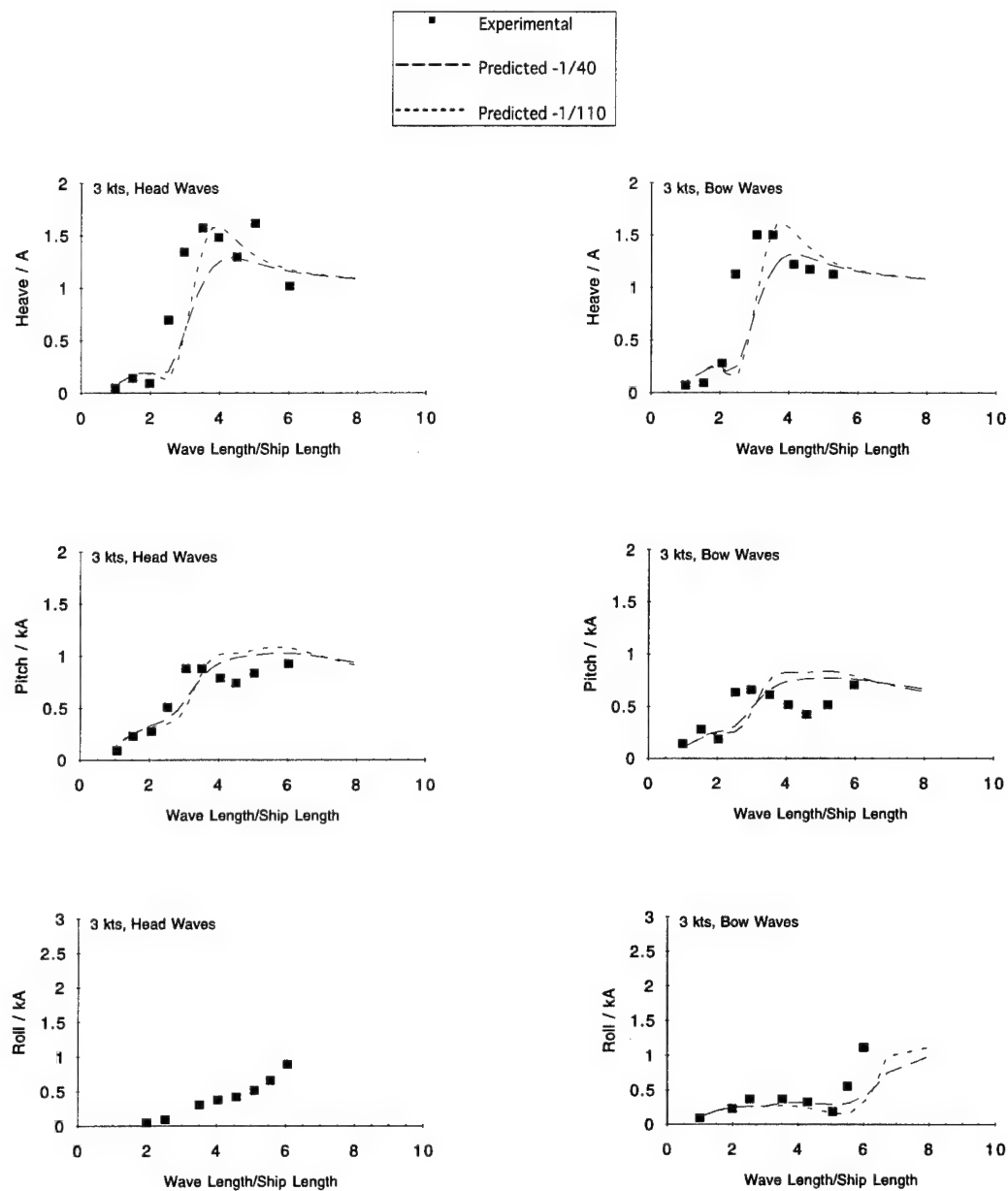
Figure 6 - Comparison of experimental and predicted motion transfer functions
for two different wave slopes for the 1981 T-AGOS at the heavy draft.

25

Figure 6 (Continued)
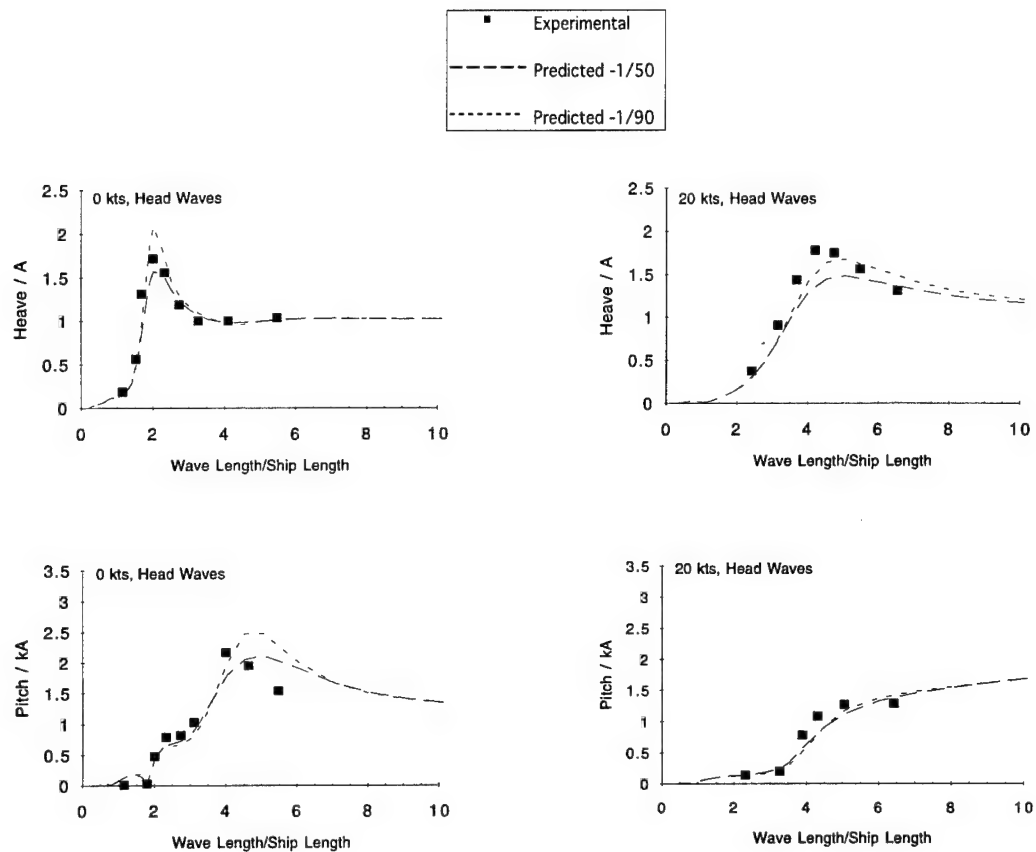
26

Figure 6 (Continued)

27
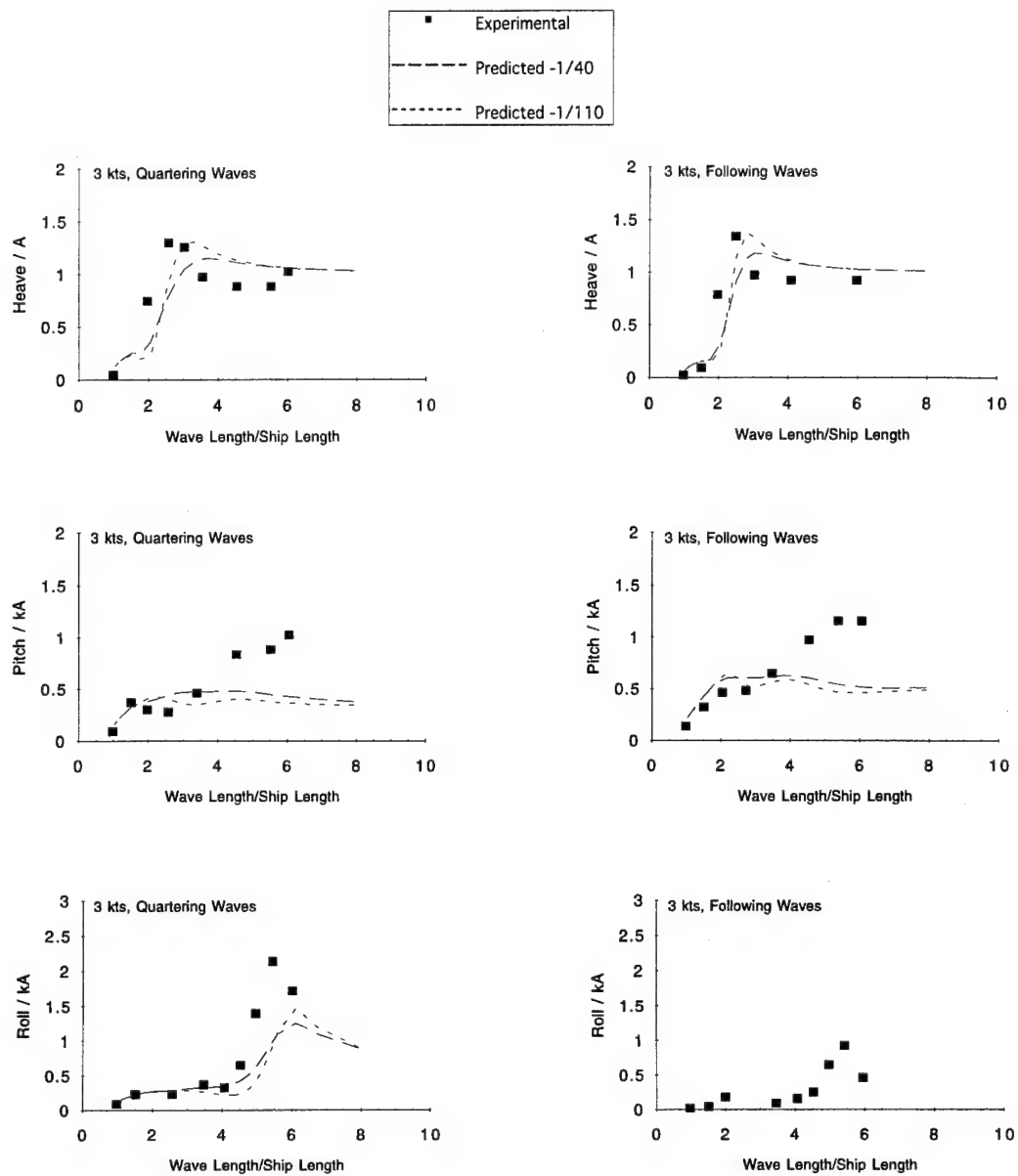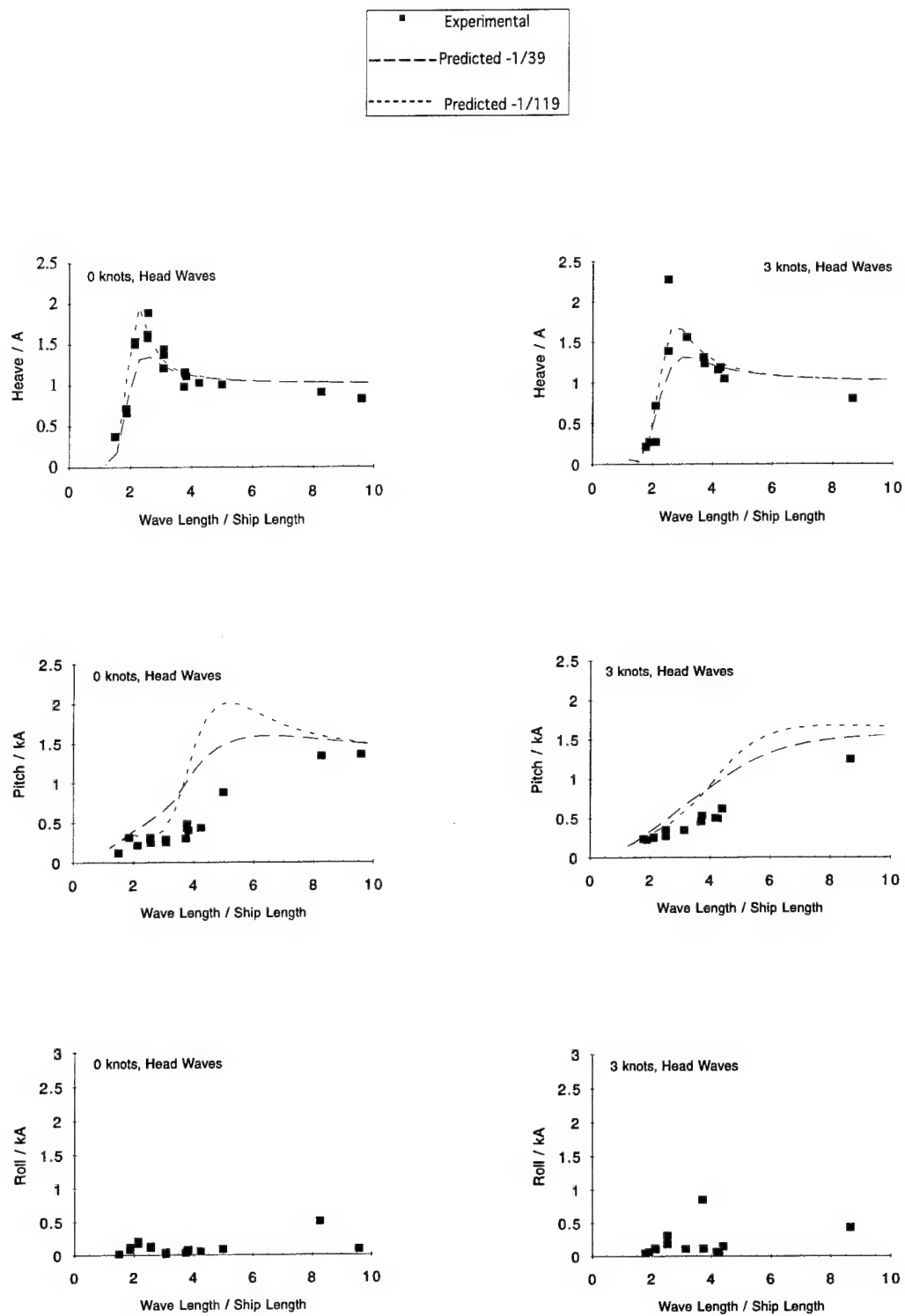
Figure 7 - Comparison of experimental and predicted motion transfer functions for two different wave slopes for the T-AGOS 19.

28

Figure 7 (Continued)

29

Figure 7 (Continued)

30

Figure 7 (Continued)

31
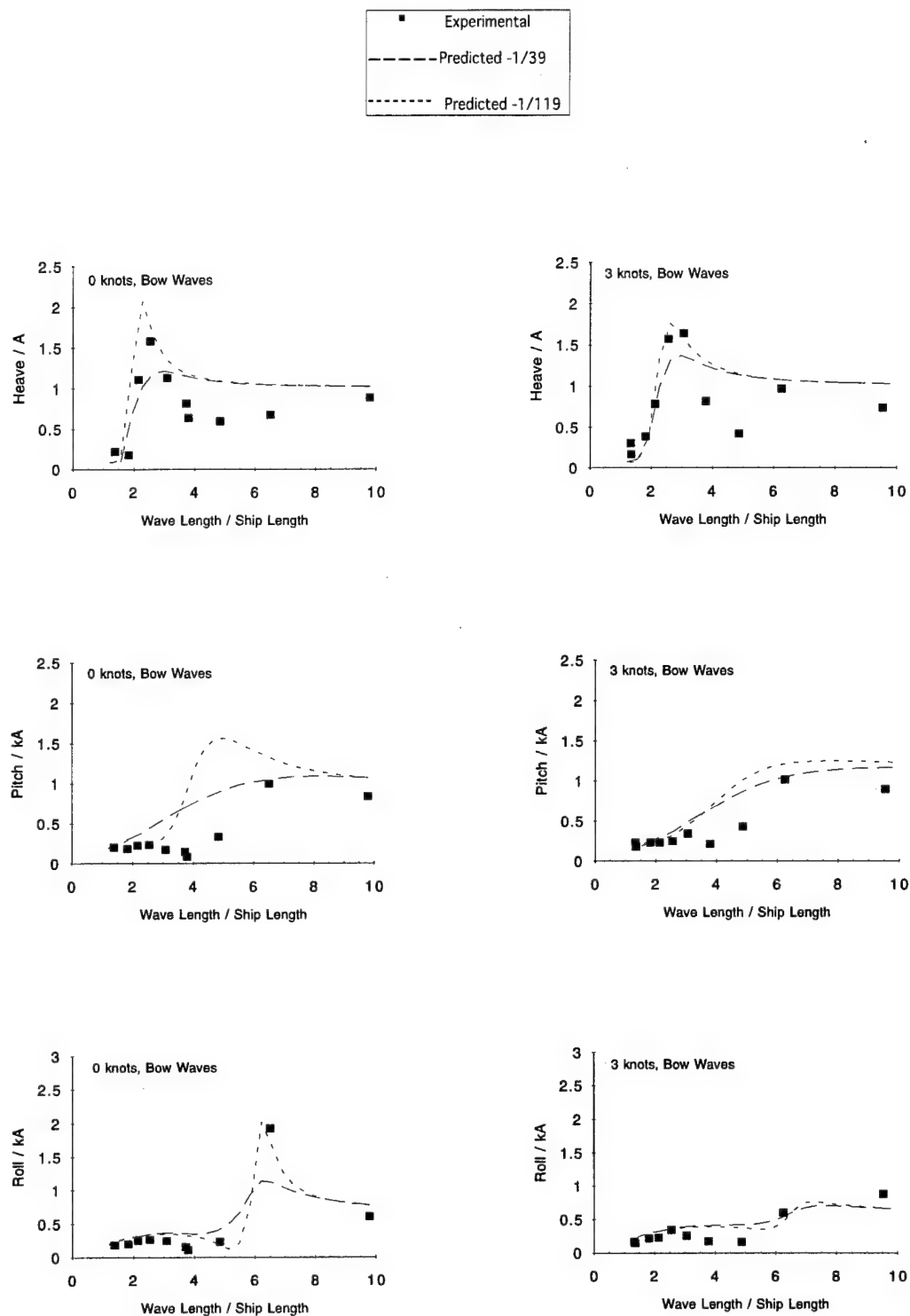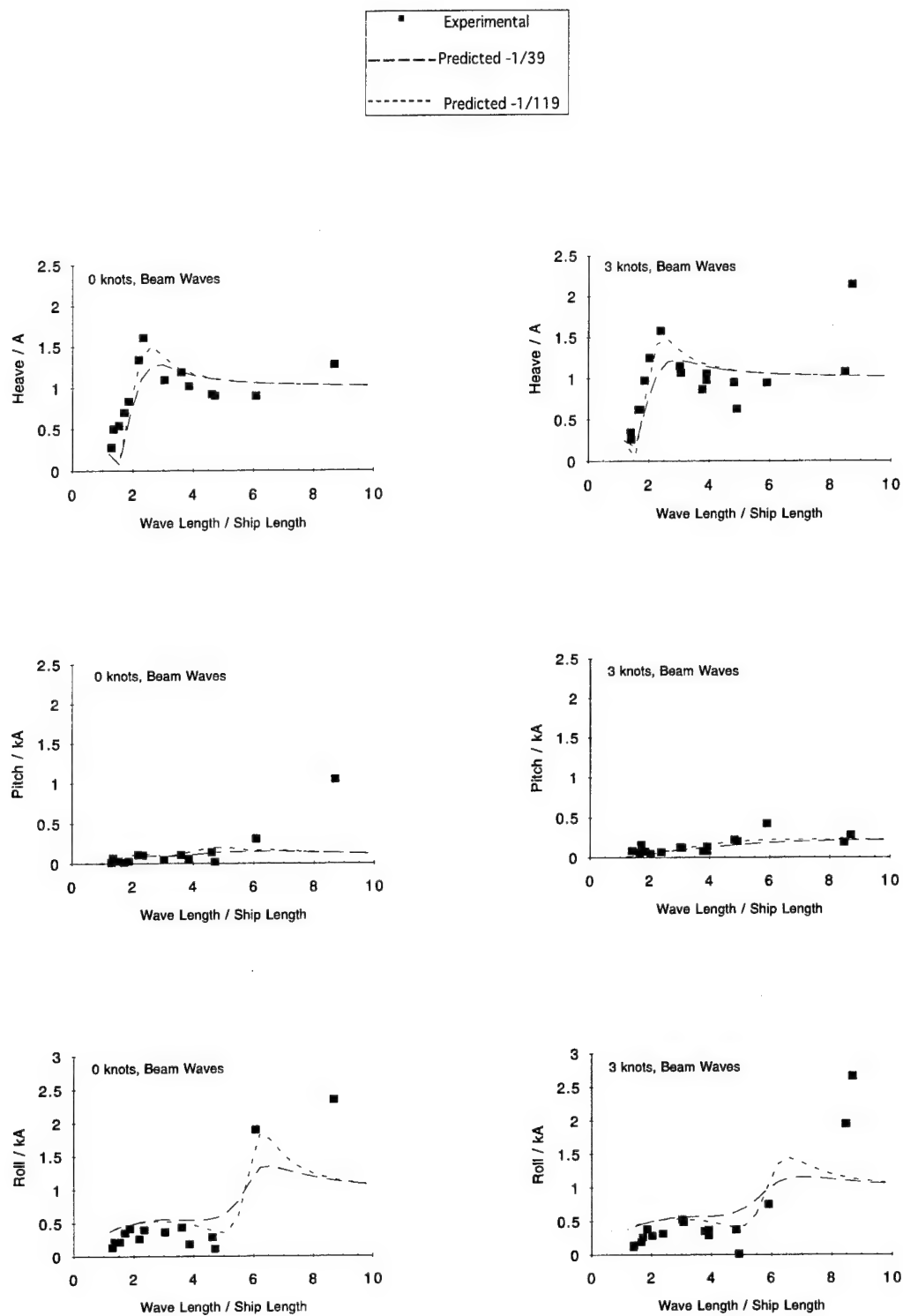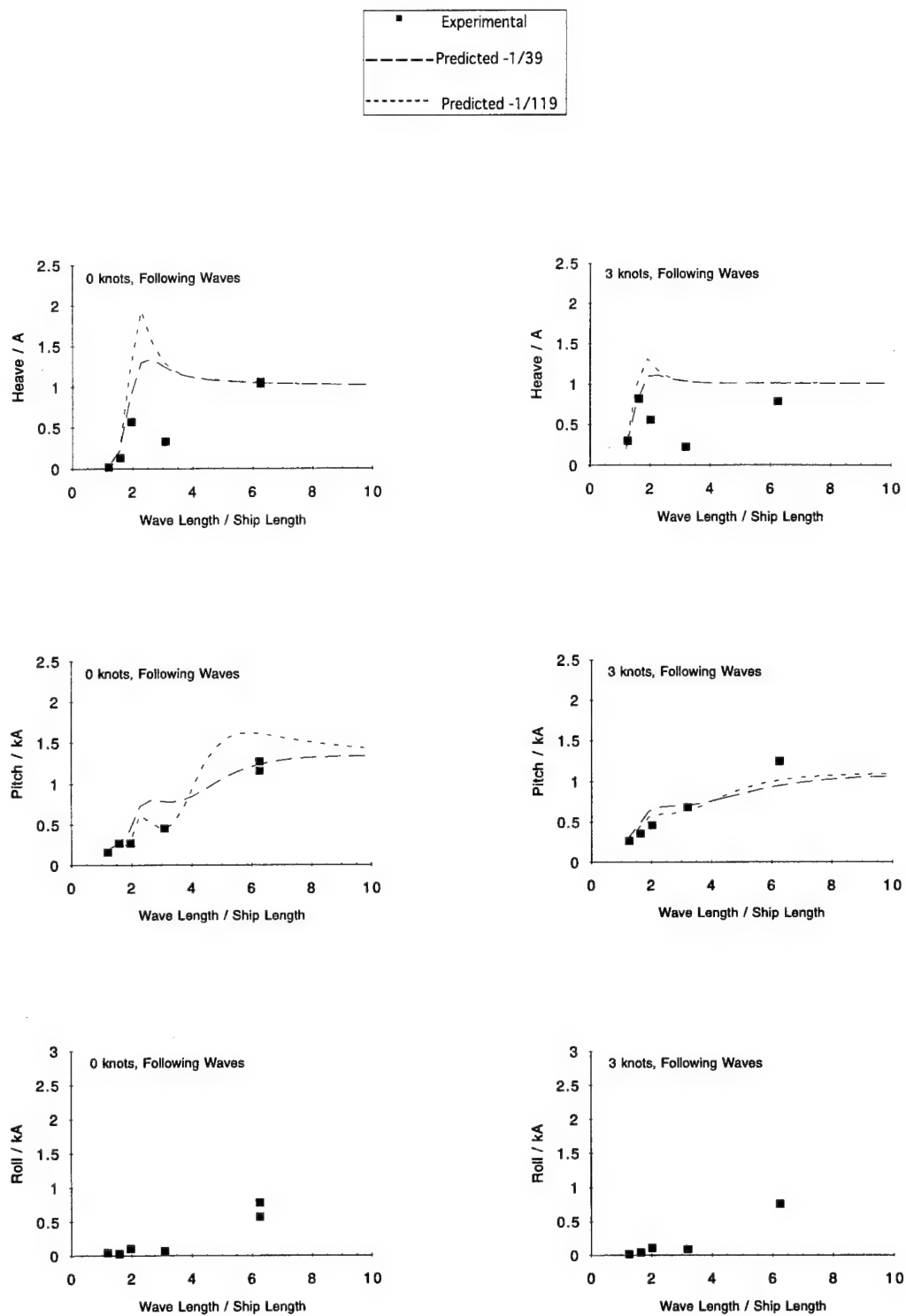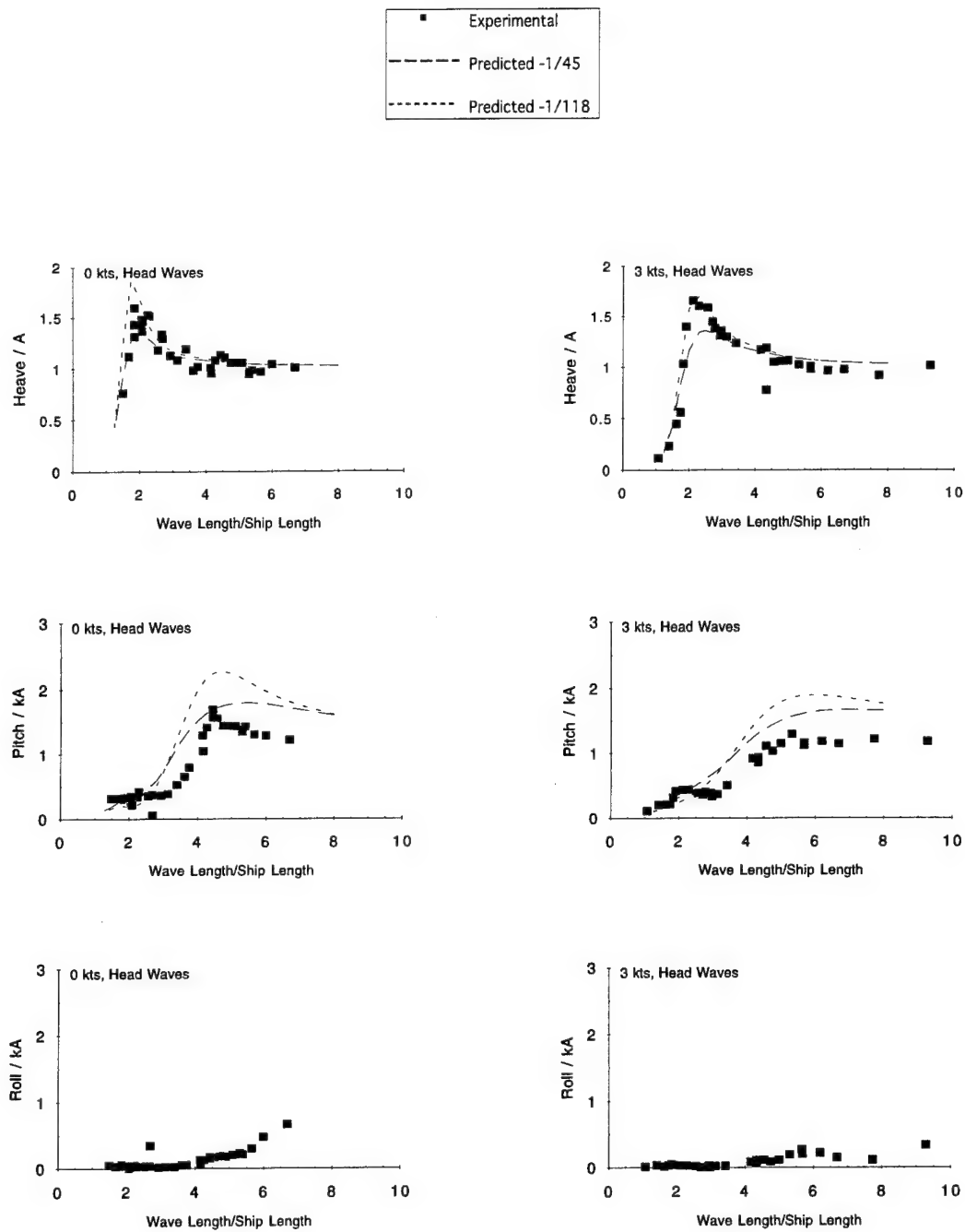
Figure 8 - Comparison of experimental and predicted motion transfer functions
for two different wave slopes for the T-AGOS 23.
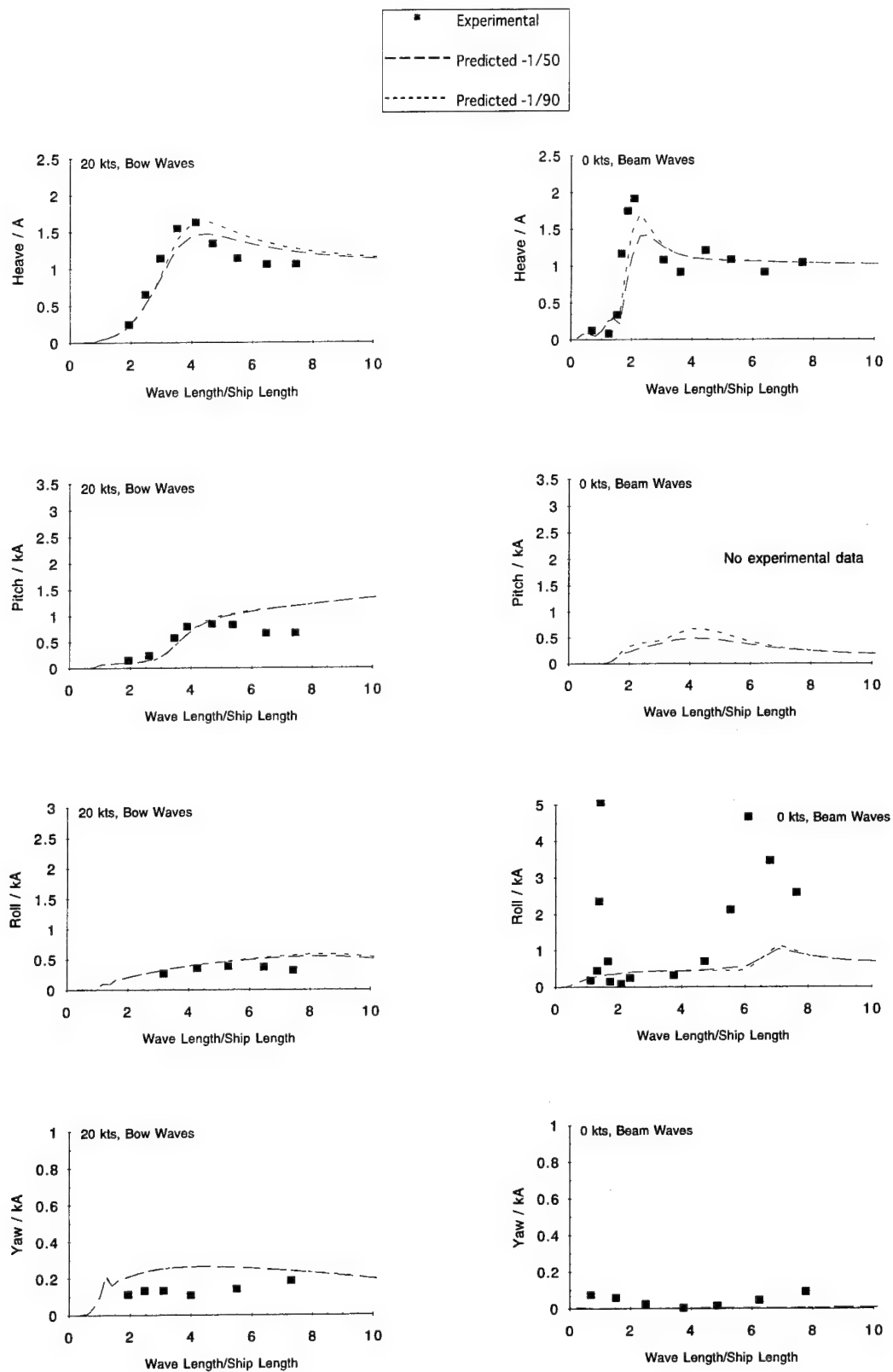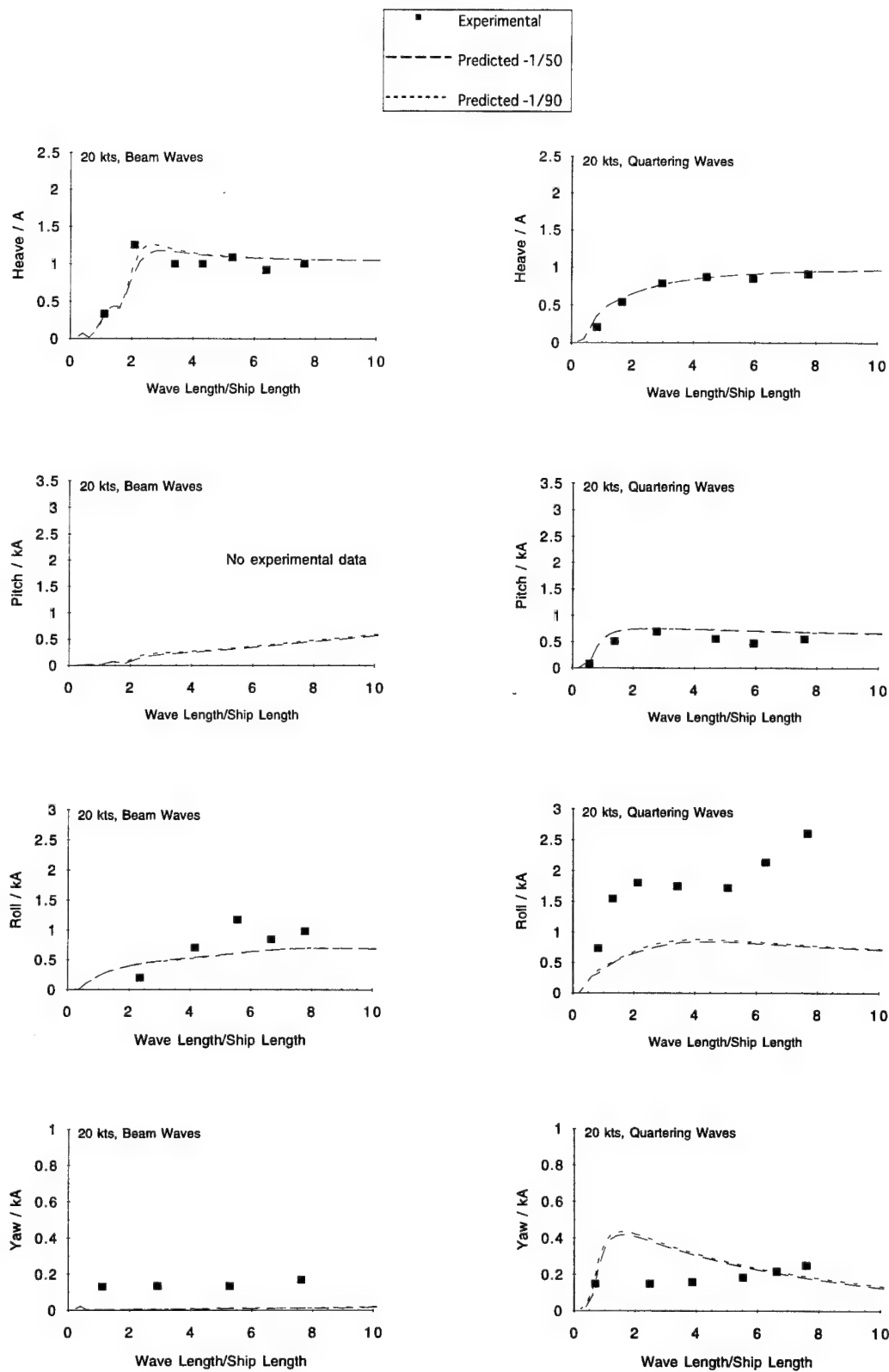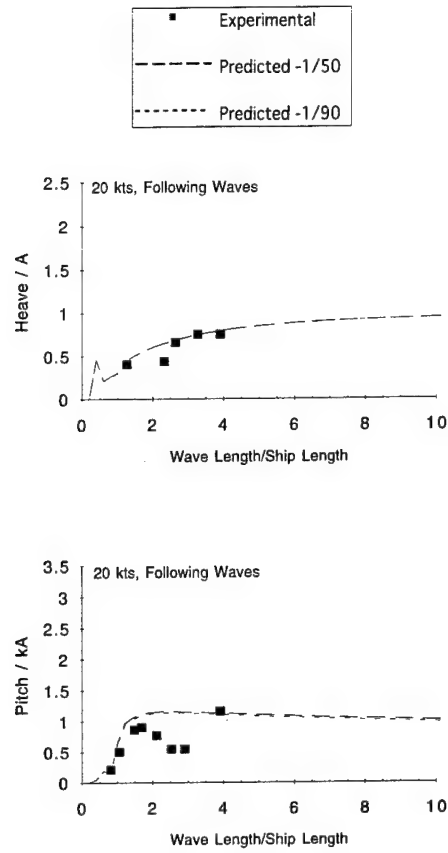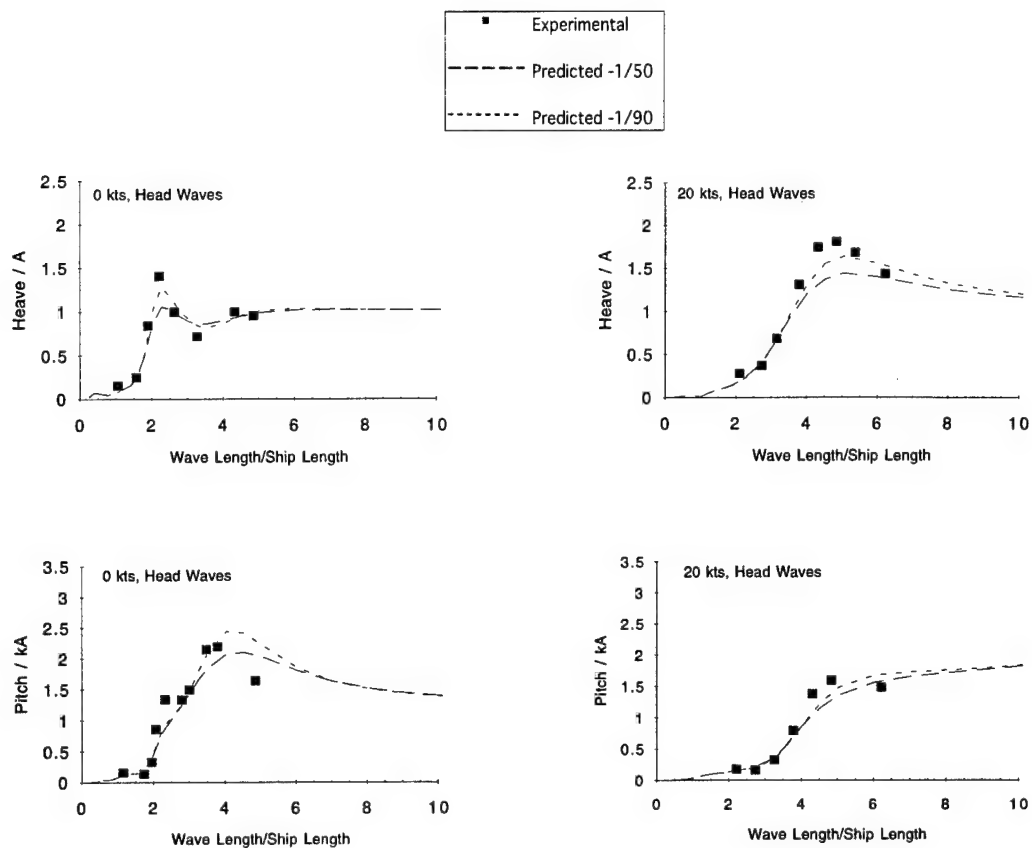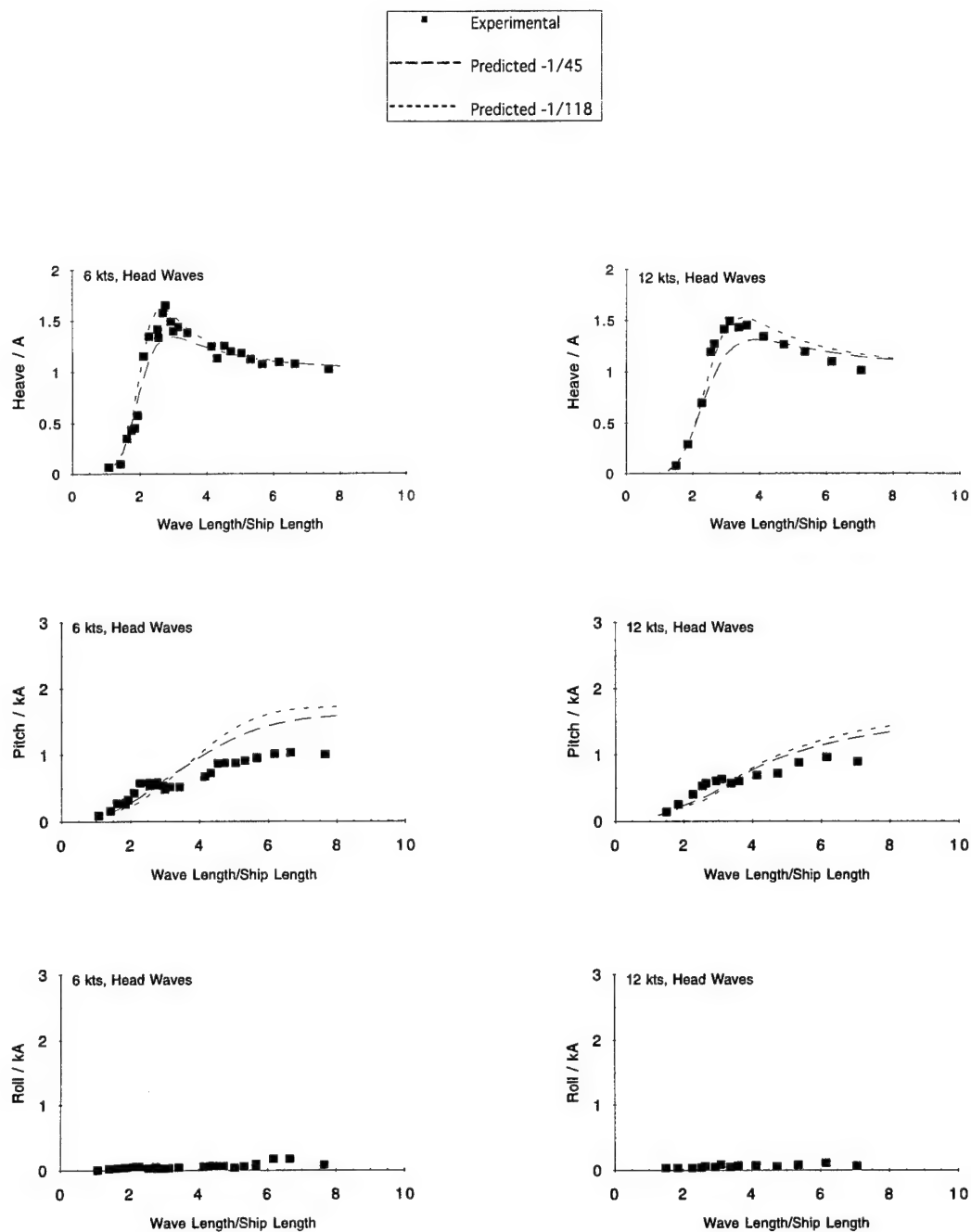
Figure 8 (Continued)
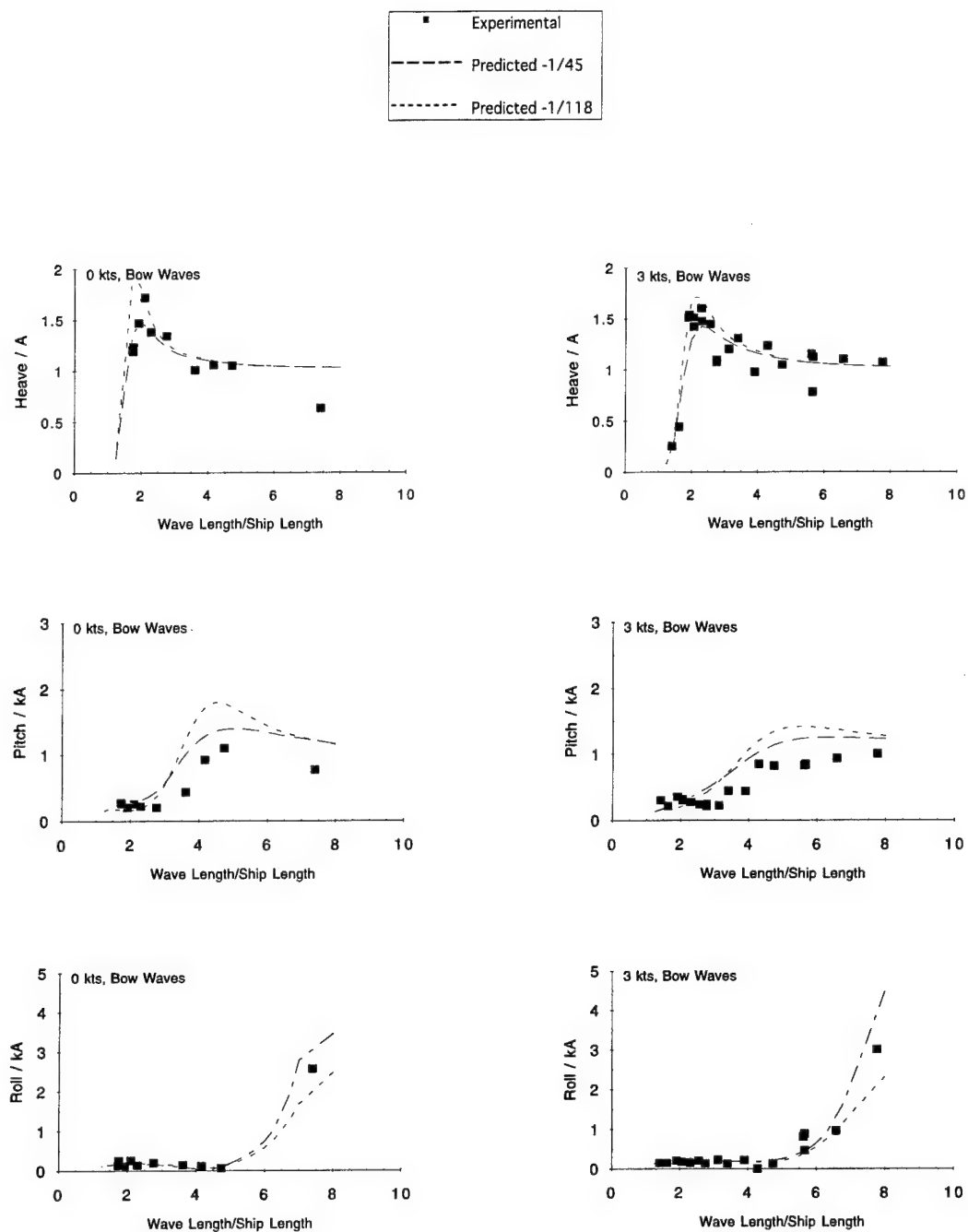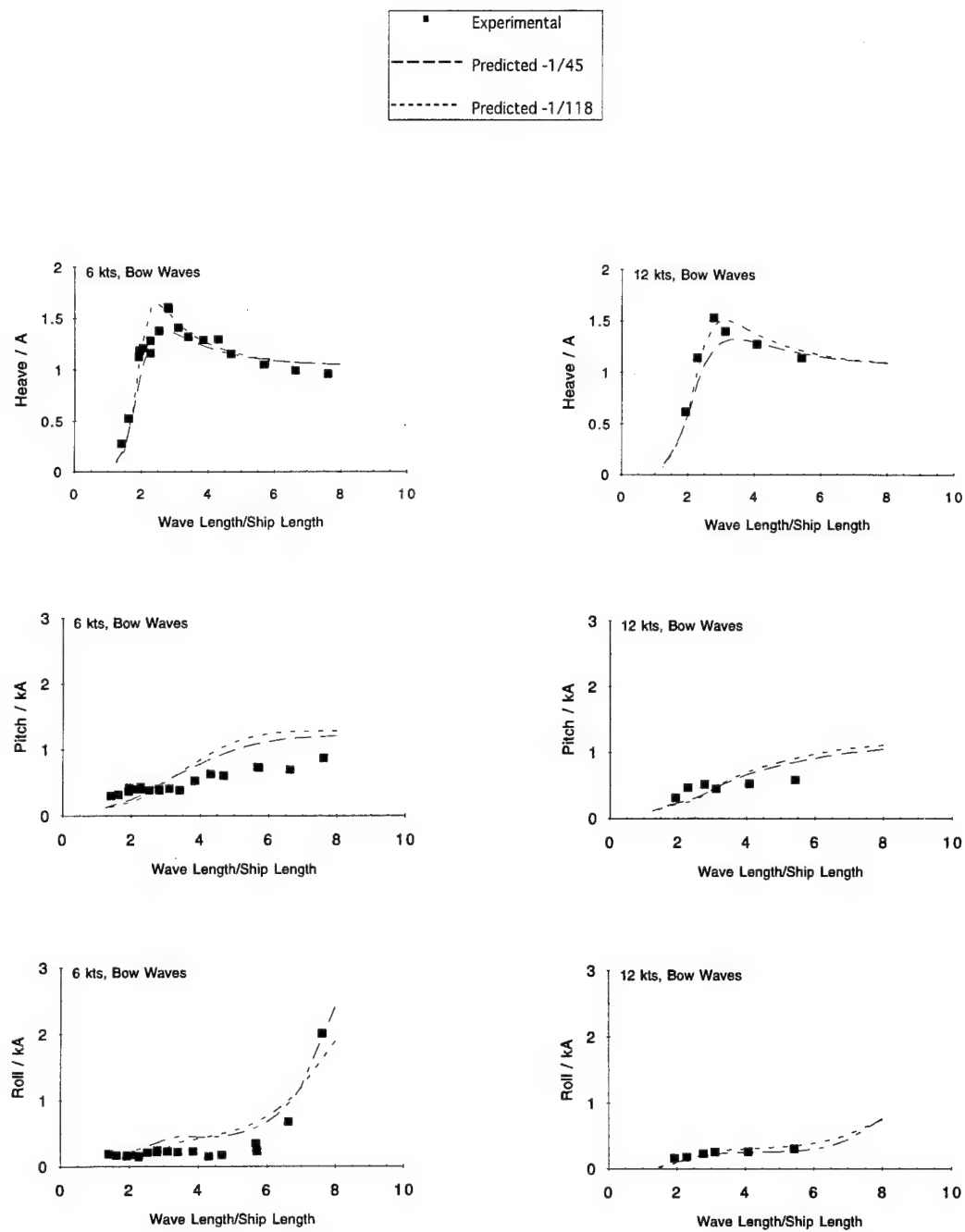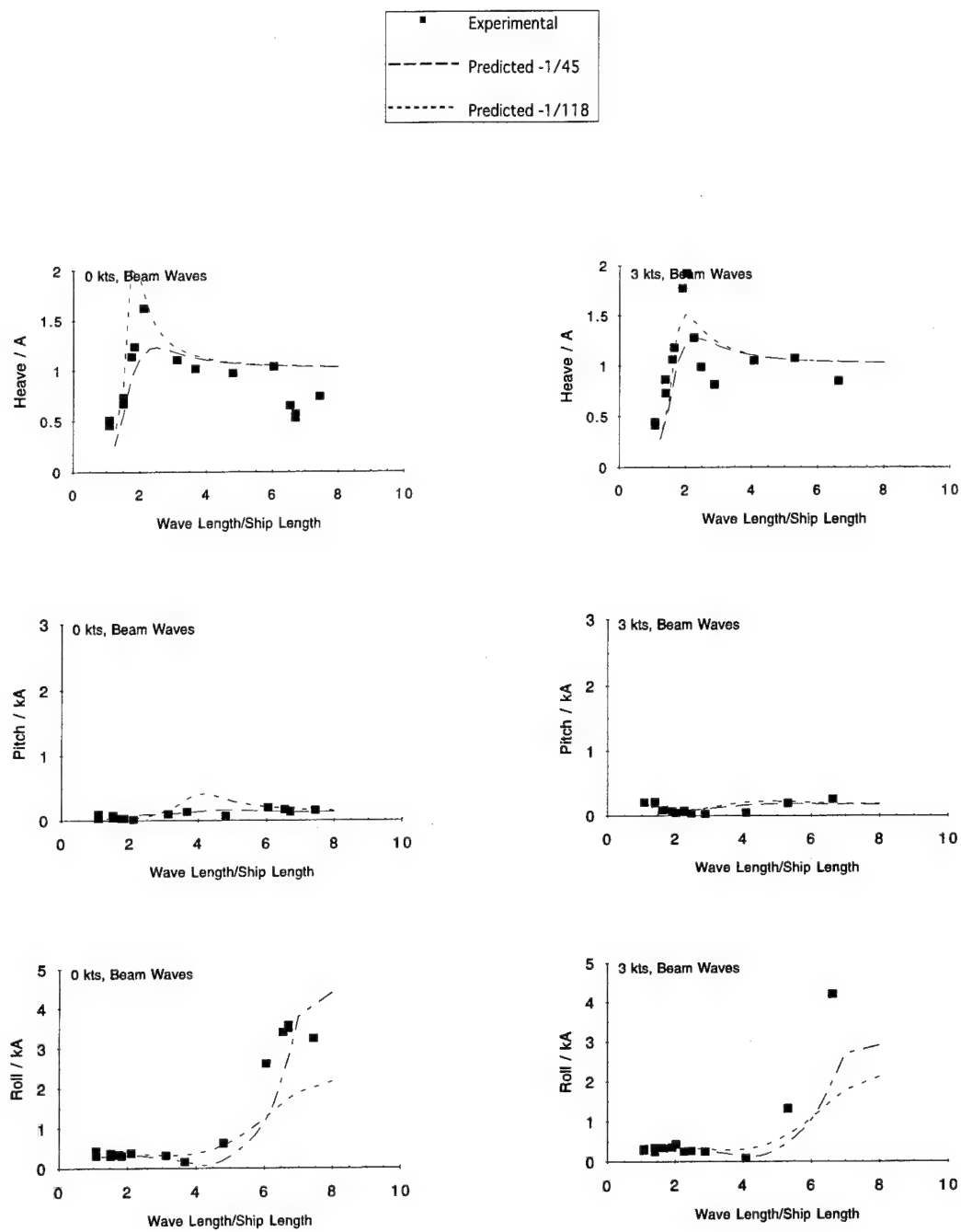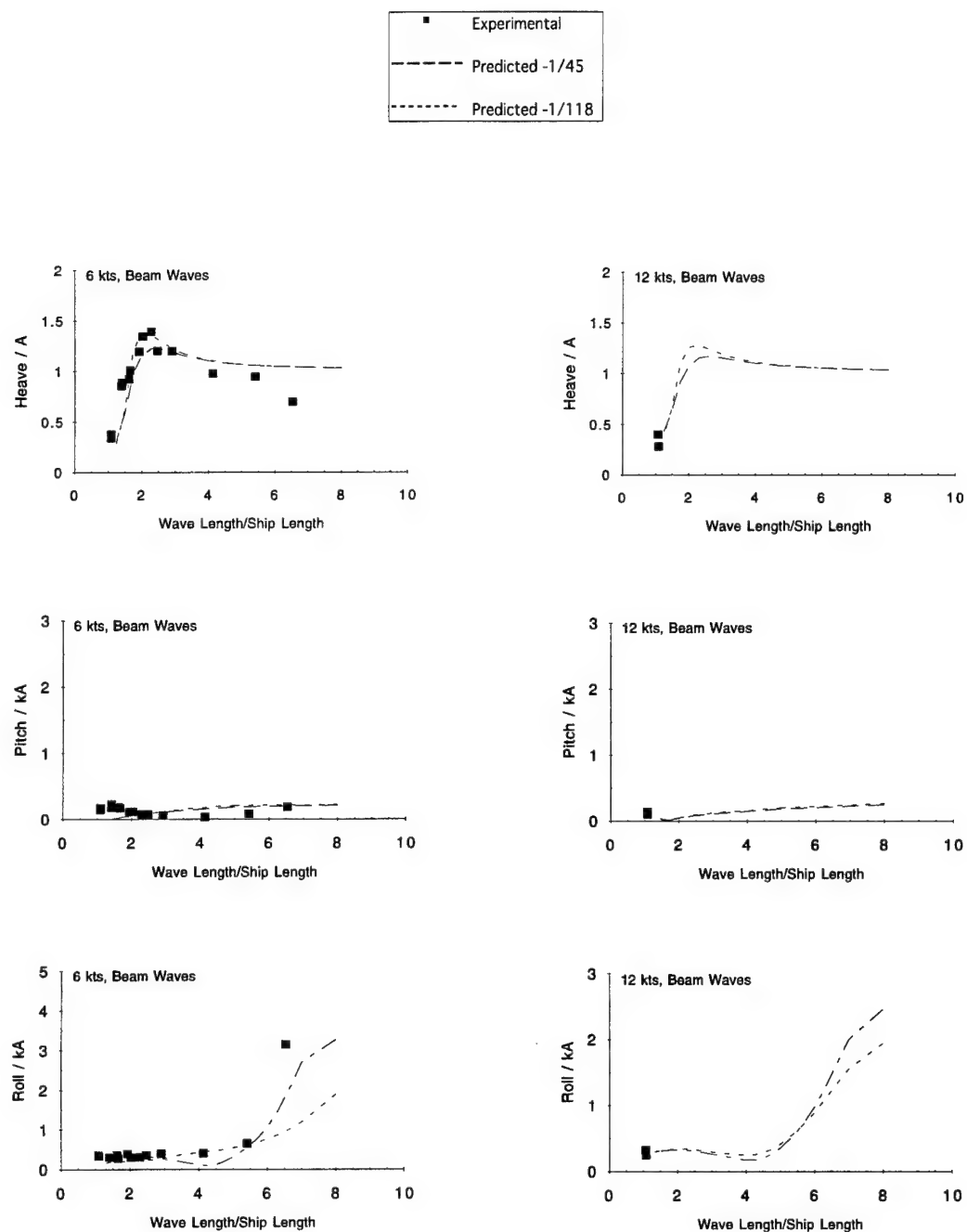
33
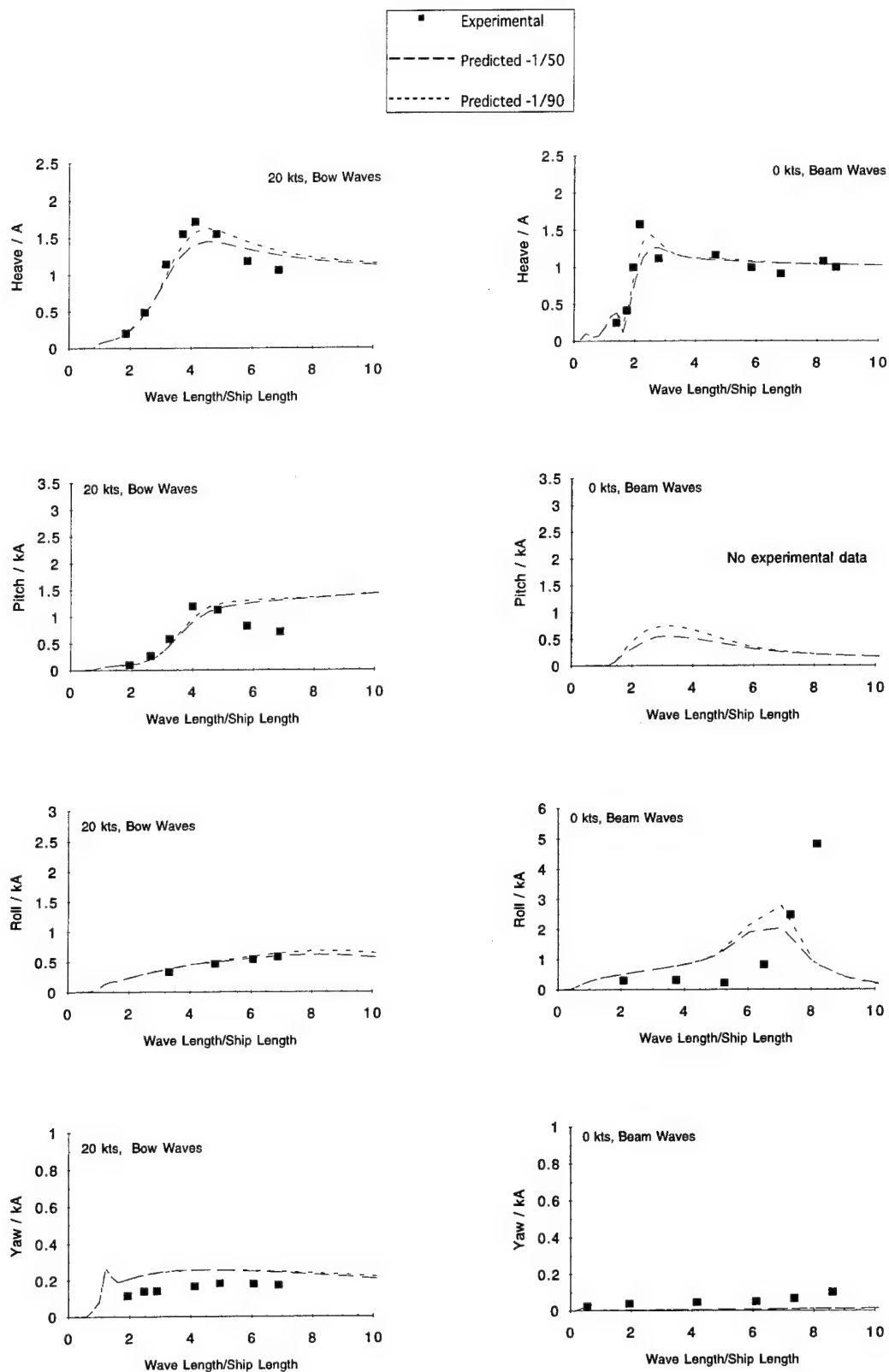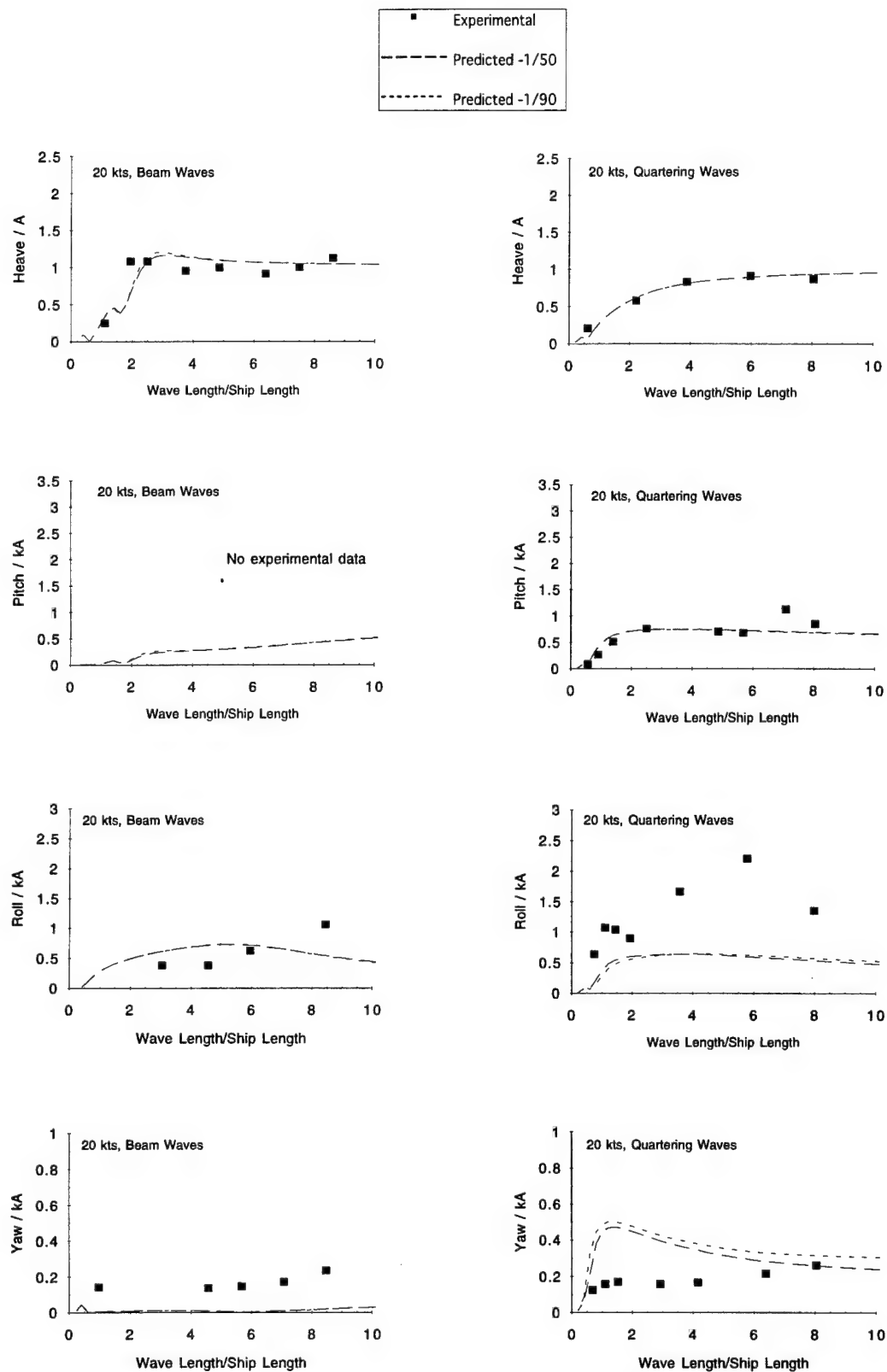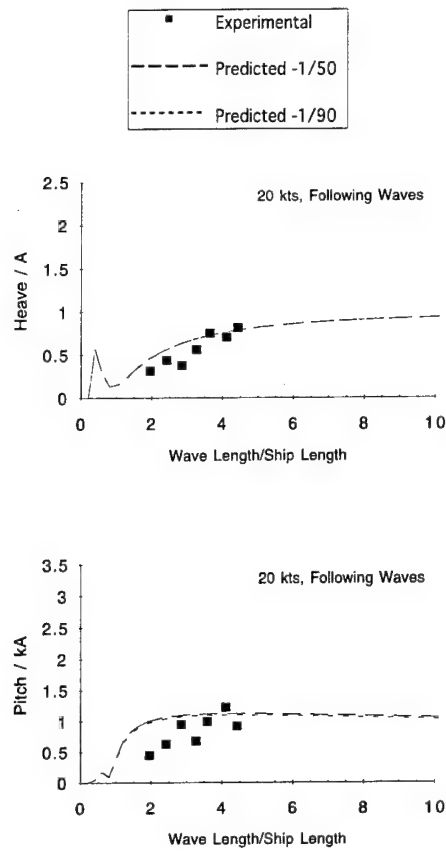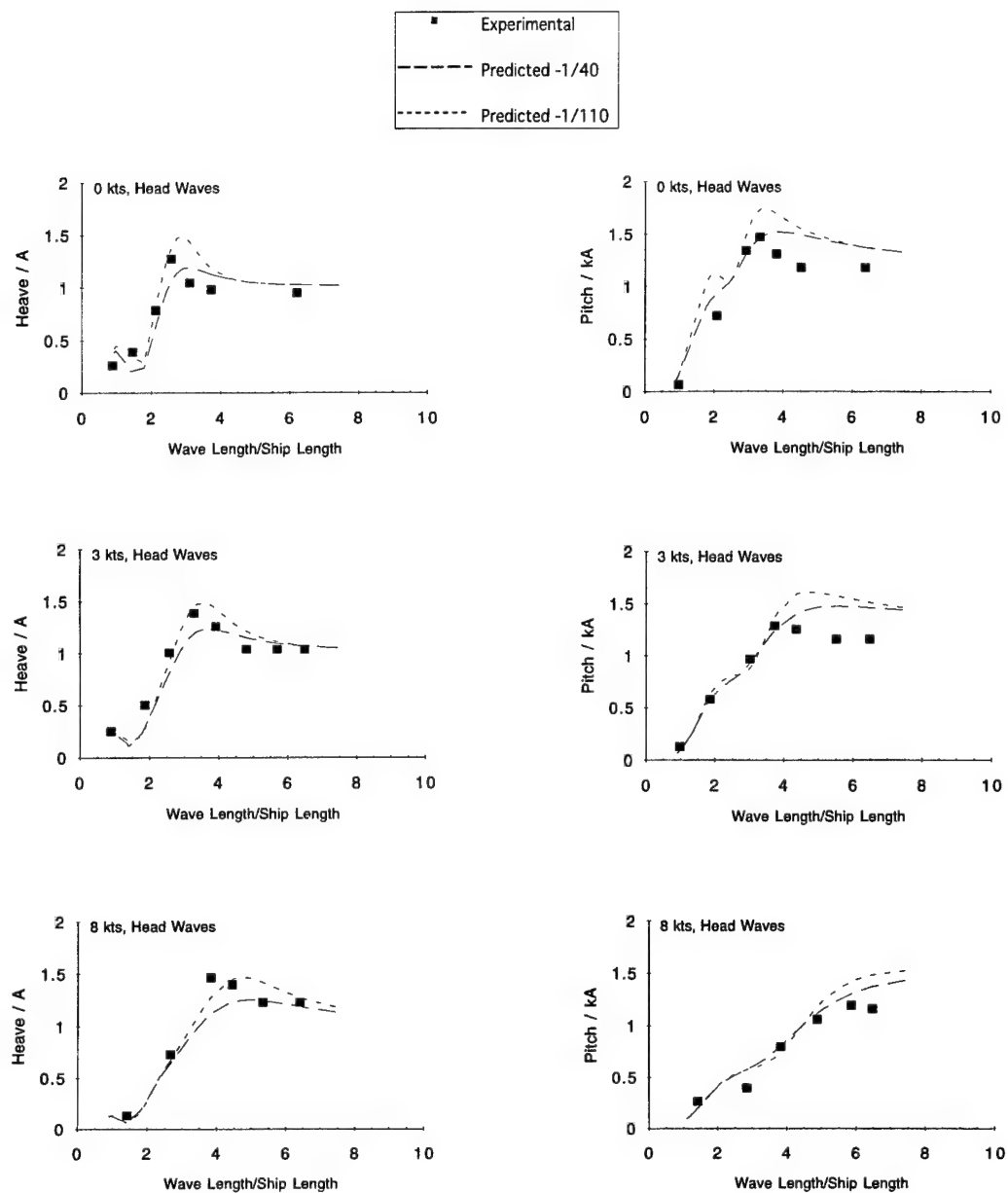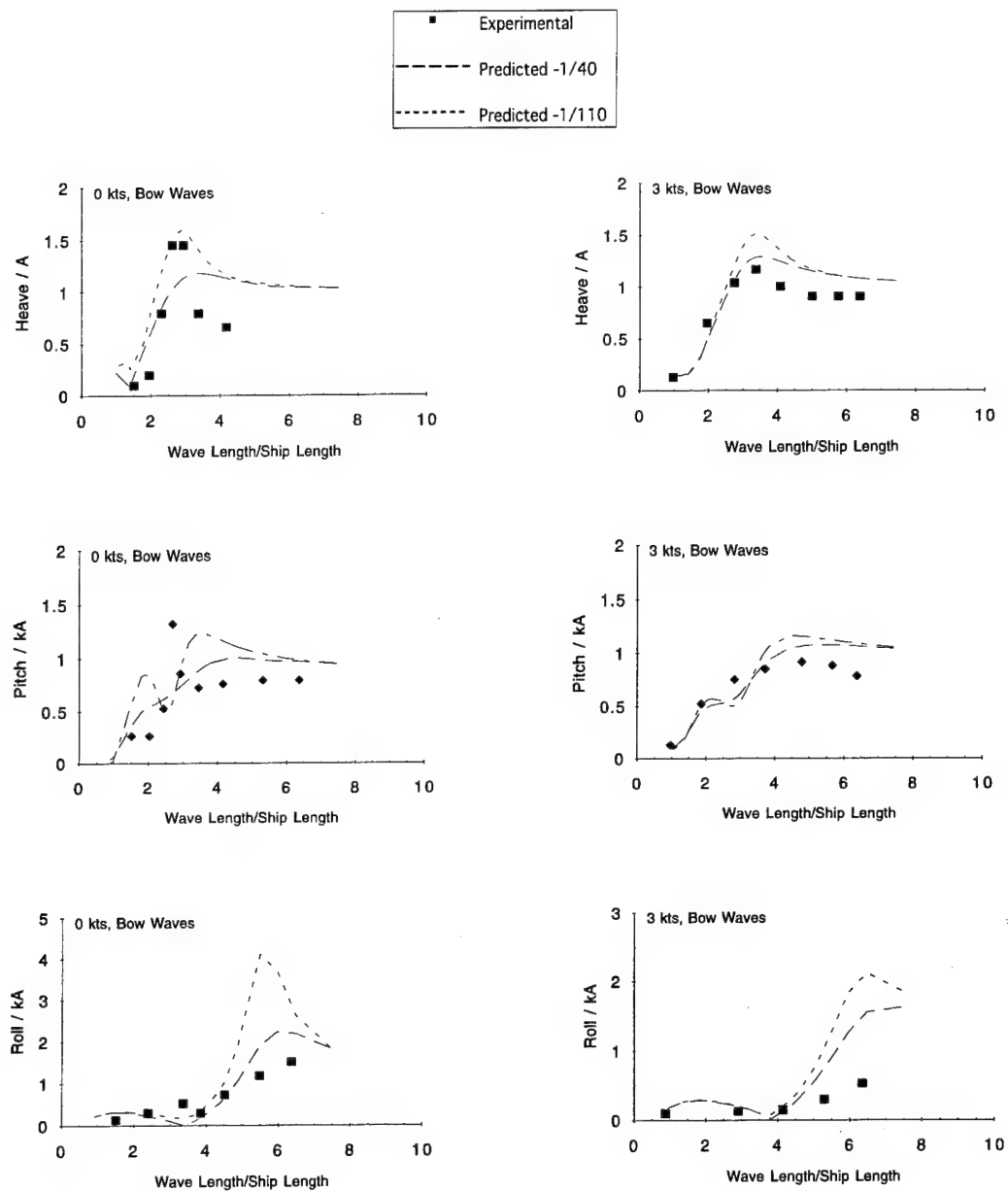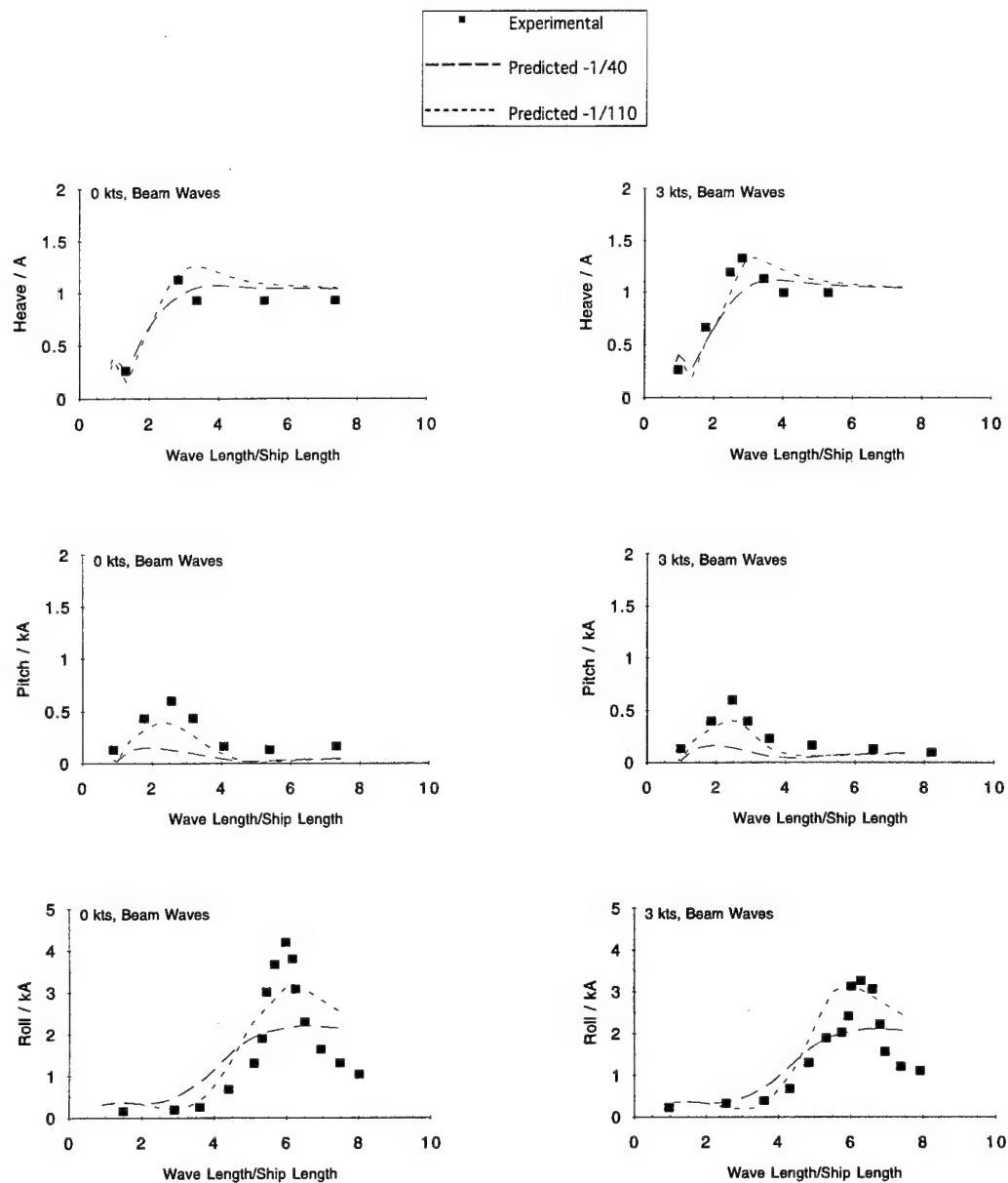
Figure 8 (Continued)
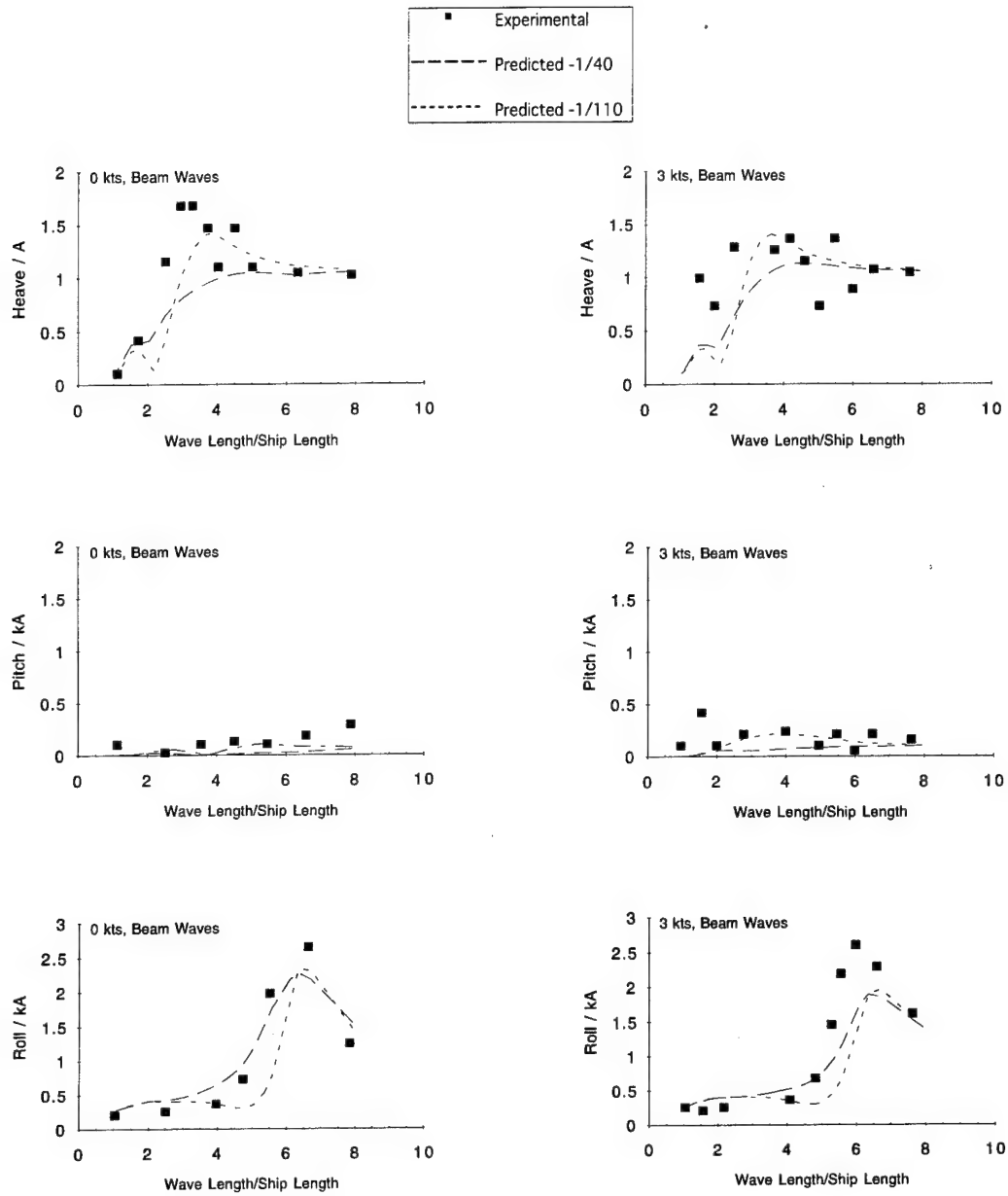
34

Figure 8 (Continued)

35

Figure 8 (Continued)

36

Figure 8 (Continued)

37

Figure 8 (Continued)

38

Figure 8 (Continued)

39

Figure 8 (Continued)

40

Figure 8 (Continued)

41
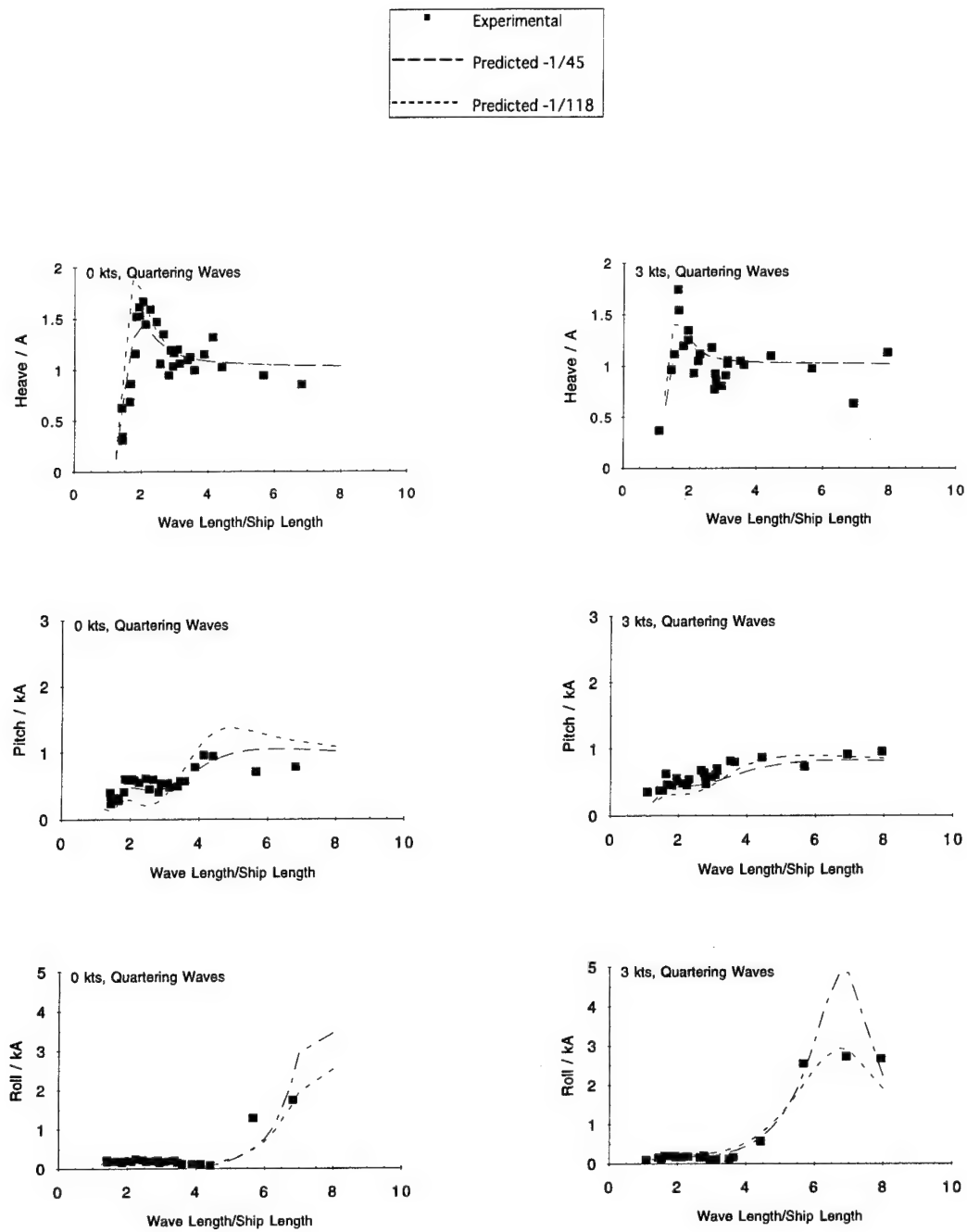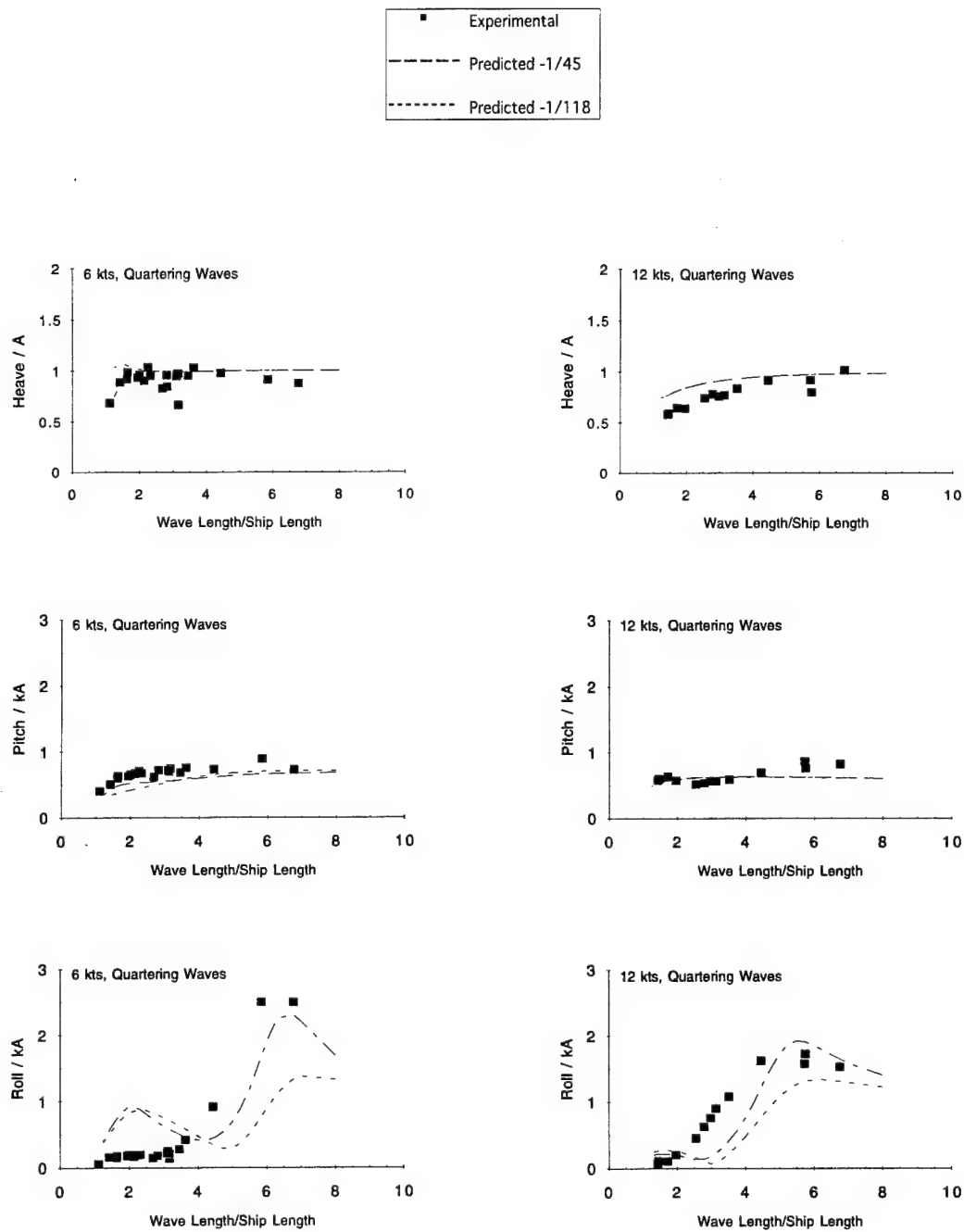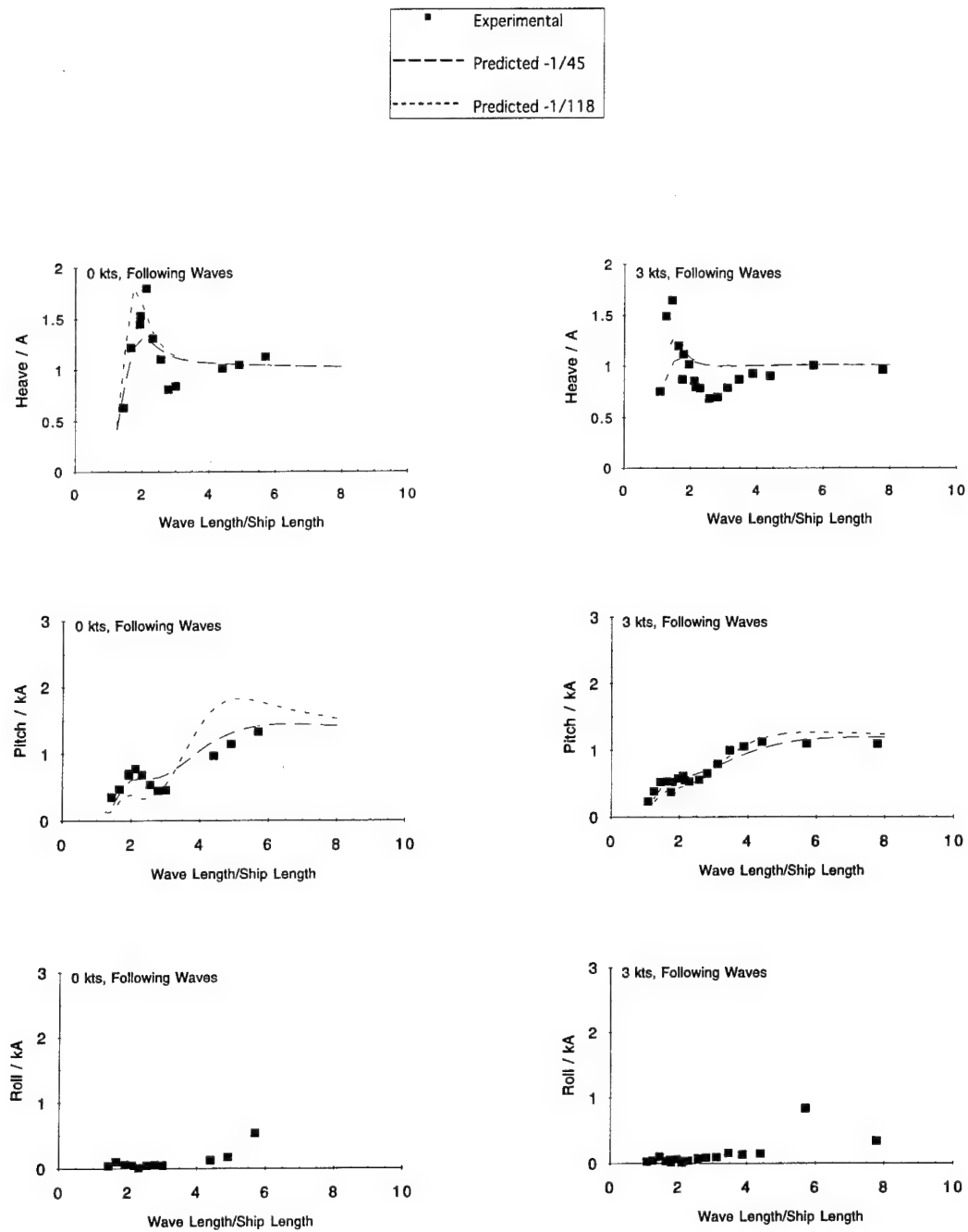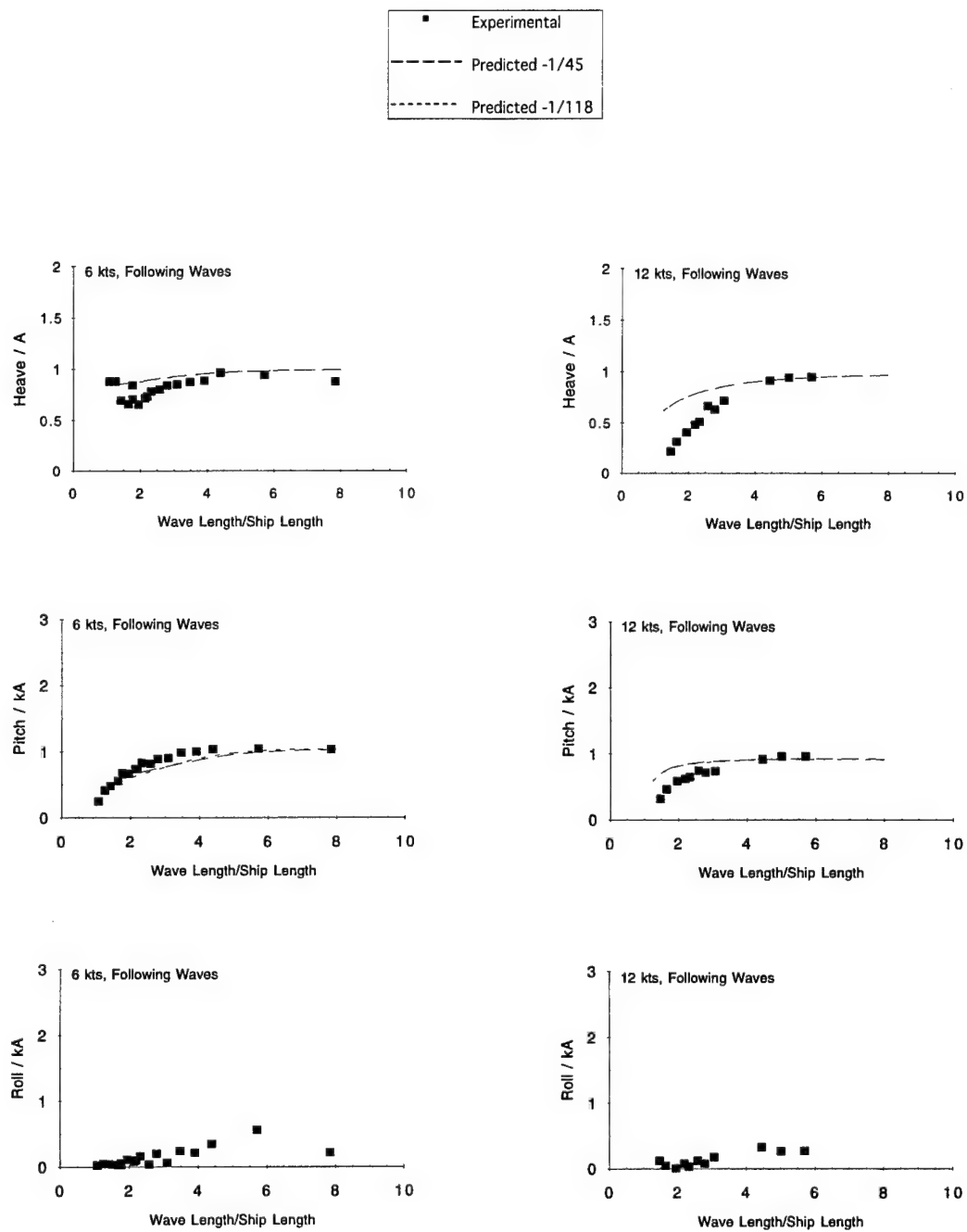
This page is intentionally left blank.

APPENDIX A - POTENTIAL FLOW TERMS

In the equations which follow, a_{kk} and b_{kk} are the two-dimensional added mass and damping coefficients. In the following three equations, integrals are taken around a two-dimensional cross section:

$$a_{22} - \frac{1}{i\omega_e} b_{22} = \rho \int_{C(x)} \phi_2 n_2 dl$$

$$a_{33} - \frac{1}{i\omega_e} b_{33} = \rho \int_{C(x)} \phi_3 n_3 dl$$

$$a_{24} - \frac{1}{i\omega_e} b_{24} = \rho \int_{C(x)} z\phi_2 n_2 dl$$

n_2 and n_3 are components of the unit vector normal to the body surface and ϕ_k is the complex velocity potential for forced oscillation in the kth mode.

Reference 3 gives the potential flow contributions to the added mass and damping. Integrals are evaluated from the tail to the nose with the origin at the longitudinal center of gravity. Contributions from both hulls are included in the integrations.

$$(A_{22})_{PF} = \int a_{22}(x)dx \qquad\qquad (B_{22})_{PF} = \int b_{22}(x)dx$$

$$(A_{24})_{PF} = \int a_{24}(x)dx \qquad\qquad (B_{24})_{PF} = \int b_{24}(x)dx$$

$$(A_{26})_{PF} = \int xa_{22}(x)dx + \frac{U}{\omega_e^2}B_{22} \qquad\qquad (B_{26})_{PF} = \int xb_{22}(x)dx - UA_{22}$$

$$(A_{33})_{PF} = \int a_{33}(x)dx \qquad\qquad (B_{33})_{PF} = \int b_{33}(x)dx$$

$$(A_{35})_{PF} = -\int xa_{33}(x)dx - \frac{U}{\omega_e^2}B_{33} \qquad\qquad (B_{35})_{PF} = -\int xb_{33}(x)dx + UA_{33}$$

$$(A_{42})_{PF} = \int a_{24}(x)dx \qquad\qquad (B_{42})_{PF} = \int b_{24}(x)dx$$

$$(A_{44})_{PF} = \int a_{44}(x)dx \qquad\qquad (B_{44})_{PF} = \int b_{44}(x)dx$$

$$(A_{46})_{PF} = \int xa_{24}(x)dx + \frac{U}{\omega_e^2}B_{24} \qquad\qquad (B_{46})_{PF} = \int xb_{24}(x)dx - UA_{24}$$

$$(A_{53})_{PF} = -\int xa_{33}(x)dx + \frac{U}{\omega_e^2}B_{33} \qquad\qquad (B_{53})_{PF} = -\int xb_{33}(x)dx - UA_{33}$$

$$(A_{55})_{PF} = \int x^2 a_{33}(x)dx + \frac{U^2}{\omega_e^2}A_{33} \qquad\qquad (B_{55})_{PF} = \int x^2 b_{33}(x)dx + \frac{U^2}{\omega_e^2}B_{33}$$

$$(A_{62})_{PF} = \int xa_{22}(x)dx - \frac{U}{\omega_e^2}B_{22} \qquad\qquad (B_{62})_{PF} = \int xb_{22}(x)dx + UA_{22}$$

$$(A_{64})_{PF} = \int xa_{24}(x)dx - \frac{U}{\omega_e^2}B_{24} \qquad\qquad (B_{64})_{PF} = \int xb_{24}(x)dx + UA_{24}$$

$$(A_{66})_{PF} = \int x^2 a_{22}dx + \frac{U^2}{\omega_e^2}A_{22} \qquad\qquad (B_{66})_{PF} = \int x^2 b_{22}dx + \frac{U^2}{\omega_e^2}B_{22}$$

With symmetry of the ship about the ship's centerline assumed, the contributions to the wave exciting forces due to potential flow are:

$$(F_2)_{PF} = -2\rho g A \int dx e^{ikx\cos\beta} \int_{C(x)} \left\{ in_2 \sin(ky\sin\beta) + \frac{k}{\omega}\left[n_2 \sin\beta\cos(ky\sin\beta) + n_3 \sin(ky\sin\beta)\right]\phi_2 \right\} e^{kz} dl$$

$$(F_3)_{PF} = 2\rho g A \int dx e^{ikx\cos\beta} \int_{C(x)} \left\{ n_3 \cos(ky\sin\beta) + i\frac{k}{\omega}\left[n_2 \sin\beta\sin(ky\sin\beta) - n_3 \cos(ky\sin\beta)\right]\phi_3 \right\} e^{kz} dl$$

$$(F_4)_{PF} = -2\rho g A \int dx e^{ikx\cos\beta}$$

$$\int_{C(x)} \left\{ i[yn_3 - zn_2]\sin(ky\sin\beta) + \frac{k}{\omega}\left[n_2 \sin\beta\cos(ky\sin\beta) + n_3 \sin(ky\sin\beta)\right]\phi_4 \right\} e^{kz} dl$$

$$(F_5)_{PF} = -2\rho g A \int dx e^{ikx\cos\beta}$$

$$\int_{C(x)} \left\{ xn_3 \cos(ky\sin\beta) + i\frac{k}{\omega}\left[x - \frac{U}{i\omega_e}\right]\left[n_2 \sin\beta\sin(ky\sin\beta) - n_3 \cos(ky\sin\beta)\right]\phi_3 \right\} e^{kz} dl$$

$$(F_6)_{PF} = -2\rho g A \int dx e^{ikx\cos\beta}$$

$$\int_{C(x)} \left\{ ixn_2 \sin(ky\sin\beta) + \frac{k}{\omega}\left[x - \frac{U}{i\omega_e}\right]\left[n_2 \sin\beta\cos(ky\sin\beta) + n_3 \sin(ky\sin\beta)\right]\phi_2 \right\} e^{kz} dl$$

Approximations for the surge wave exciting force and surge wave exciting force due to pitch are:

$$(F_1)_{PF} = -2i\rho g A k \cos\beta \iiint e^{kz+ikx\cos\beta} \cos(ky\sin\beta) dz dy dx$$

$$(F_{51})_{PF} = 2i\rho g A k \cos\beta \iiint z e^{kz+ikx\cos\beta} \cos(ky\sin\beta) dz dy dx$$

APPENDIX B - CROSS FLOW DRAG AND BODY LIFT TERMS

Lift and Cross Flow Drag Vertical Plane Force

From Thwaites[4], the vertical force, F_Z, for an inclined body at α, a moderate angle of incidence relative to the flow, is:

$$F_Z = \frac{\rho}{2} A_V \left(U^2 a_{0V} \alpha + C_{DV} w|w| \right) \tag{B.1}$$

where ρ is the mass density of the fluid, A_V is the area projected in the vertical plane, U is the forward speed of the ship, a_{0V} is the lift coefficient, α is the angle of incidence of flow, C_{DV} is the cross flow drag coefficient and w is the relative vertical fluid velocity with respect to the body. From Figure B.1 it follows that

$$\sin(\alpha - \xi_5) = \frac{-z_b}{U}$$

$$w = -z_b$$

so that, for small angles,

$$w = U(\alpha - \xi_5)$$
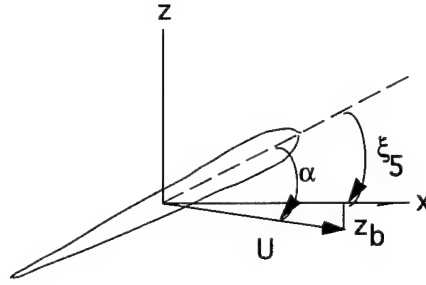
Figure B.1. A sketch of a body moving with respect to the fluid in the vertical plane.

For an arbitrary point (x,y,z),

$$w = \dot{\xi}_3 - x\dot{\xi}_5 + y\dot{\xi}_4 - \dot{\zeta}_v(x,y,z)$$

where the vertical velocity of the fluid induced by the incoming wave is

$$\dot{\zeta}_V = \frac{\partial \phi_0}{\partial z} e^{-i\omega_e t}$$

and ϕ_0, the complex velocity potential for the incident wave, is defined by

$$\phi_0 = -\frac{igA}{\omega} e^{kz + ikx\cos\beta - iky\sin\beta}$$

where g is the acceleration due to gravity, A is the wave amplitude, ω is the wave frequency, k is the wave number, β is the heading of the ship relative to the wave and ω_e is the wave encounter frequency. Consequently,

$$w = \dot{\xi}_3 - x\dot{\xi}_5 + y\dot{\xi}_4 + i\omega Ae^{kz+ikx\cos\beta-iky\sin\beta} \quad \text{and} \tag{B.2}$$

$$\alpha = \xi_5 + \left(\dot{\xi}_3 - x\dot{\xi}_5 + y\dot{\xi}_4 + i\omega Ae^{kz+ikx\cos\beta-iky\sin\beta} \right) / U \tag{B.3}$$

Equations (B.2) and (B.3) can be substituted in Equation (B.1) to define F_V.

45

<u>Lift and Cross Flow Drag Transverse Plane Force</u>

Applying Thwaites'[4] expression to the transverse plane, the horizontal force F_Y for a body with a moderate drift angle is:

$$F_Y = \frac{\rho}{2} A_H \left(U^2 a_{0H} \gamma + C_{DH} v|v| \right) \tag{B.4}$$

where A_H is the area projected in the horizontal plane, a_{0H} is the lift coefficient, γ is the angle of incidence of flow, C_{DH} is the cross flow drag coefficient, and v is the relative fluid velocity with respect to the body. Referring to Figure B.2,

$$\sin(-\gamma + \xi_6) = \frac{-y_b}{U}$$

$$v = -y_b$$

so that, for small angles,

$$v = -U(\gamma - \xi_6)$$
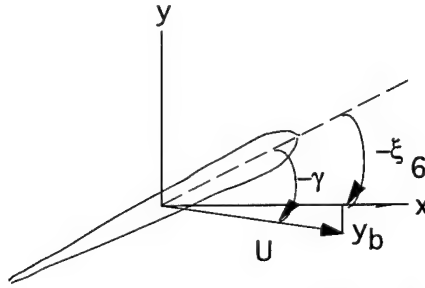
Figure B.2.   A sketch of a body moving with respect to the fluid in the transverse plane.

For an arbitrary point (x,y,z),

$$v = \dot{\xi}_2 + x\dot{\xi}_6 - z\dot{\xi}_4 - \dot{\zeta}_H(x,y,z)$$

where the horizontal velocity of the fluid induced by the incoming wave is

$$\dot{\zeta}_H = \frac{\partial \phi_0}{\partial y} e^{-i\omega_e t}$$

Consequently,

$$v = \dot{\xi}_2 + x\dot{\xi}_6 - z\dot{\xi}_4 + \omega A \sin\beta \, e^{kz + ikx\cos\beta - iky\sin\beta} \tag{B.5}$$

$$\gamma = \xi_6 - \left(\dot{\xi}_2 + x\dot{\xi}_6 - z\dot{\xi}_4 + \omega A \sin\beta \, e^{kz + ikx\cos\beta - iky\sin\beta} \right) / U \tag{B.6}$$

Equations (B.5) and B.(6) can be substituted in Equation (B.4) to define F_Y.

<u>Lift and Cross Flow Drag Moments</u>

The roll , pitch, and yaw moments (M_X, M_Y, M_Z) can be defined as:

$$M_X = yF_Z + zF_Y \tag{B.7}$$

$$M_Y = -xF_Z \tag{B.8}$$

$$M_Z = xF_Y \tag{B.9}$$

Evaluation of Body Cross Flow Drag and Lift Components

Equations (B.2) and (B.3) are substituted in equation (B.1) and equations (B.5) and (B.6) are substituted in equation (B.4) and applied along the ship. When terms are collected depending on whether they include velocities, displacements, or terms related to the incident wave potential, contributions to damping, restoring coefficients, and wave exciting forces are identified.

In order to evaluate the forces F_Y, F_Z, M_X, M_Y and M_Z for the entire ship, the terms which are defined in equations (B.1) to (B.9) are integrated along the port and starboard hulls. For example,

$$F_Z = \frac{\rho}{2} \int \left\{ F_{Z_P} + F_{Z_S} \right\} dx$$

This equation is expanded with the lift and drag coefficients assumed to vary longitudinally. Terms associated with cross flow drag coefficients include terms of the form $\dot{b}|\dot{b}|$, where $\dot{b}$ is a velocity. These terms are nonlinear; consequently, in order to be able to solve these terms in the linear domain, equilinearization is applied. That is, for any harmonic motion given by $b = b_0 \cos \omega_e t$, $\dot{b}|\dot{b}|$ can be approximated in the following manner[3]:

$$\dot{b}|\dot{b}| \approx \frac{8}{3\pi} \omega_e \dot{b} b_0$$

For the port hull F_Z is applied at $(x, S_D, -d_1)$ and for the starboard hull it is applied at $(x, -S_D, -d_1)$ where S_D is the distance from the ship centerline to the strut centerline, and d_1 is the distance between the calm waterline and the maximum beam of the hull or half the draft for sections with no lower hull. The projected area A_V in equation (B.1) is replaced by integrating d_H, the horizontal diameter of the lower hull. When equilinearization is applied, and terms are grouped, F_Z produces the following contributions:

$$(B_{33})_{BL+BCD} = \rho U \int a_{0V} d_H dx + \frac{\rho}{2} \frac{8}{3\pi} \int d_H \left(C_{DVP} |w_P| + C_{DVS} |w_S| \right) dx$$

$$(B_{34})_{BL+BCD} = \frac{\rho}{2} \frac{8}{3\pi} \int S_D d_H \left(C_{DVP} |w_P| - C_{DVS} |w_S| \right) dx$$

$$(B_{35})_{BL+BCD} = -\rho U \int x a_{0V} d_H dx - \frac{\rho}{2} \frac{8}{3\pi} \int x d_H \left(C_{DVP} |w_P| + C_{DVS} |w_S| \right) dx$$

$$(C_{35})_{BL+BCD} = \rho U^2 \int a_{0V} d_H dx$$

$$(F_3)_{BL+BCD} = -i\rho U \omega A \int a_{0V} d_H \cos(k S_D \sin\beta) e^{-kd_1 + ikx \cos\beta} dx$$

$$\qquad -i\omega A \frac{\rho}{2} \frac{8}{3\pi} \int d_H \left(C_{DVP} |w_P| e^{-ikS_D \sin\beta} + C_{DVS} |w_S| e^{ikS_D \sin\beta} \right) e^{-kd_1 + ikx \cos\beta} dx$$

where a_{0V}, C_{DVP} and C_{DVS} are the vertical lift, port hull vertical cross flow drag and starboard hull cross flow drag coefficients. The relative vertical velocities at the port and starboard hulls are:

$$w_P = \dot{\xi}_3 - x\dot{\xi}_5 + S_D \dot{\xi}_4 + i\omega A e^{-kd_1 + ikx \cos\beta - ikS_D \sin\beta}$$

$$w_S = \dot{\xi}_3 - x\dot{\xi}_5 - S_D \dot{\xi}_4 + i\omega A e^{-kd_1 + ikx \cos\beta + ikS_D \sin\beta}$$

Similarly,

$$F_Y = \frac{\rho}{2} \int \left\{ F_{Y_P} + F_{Y_S} \right\} dx$$

47

is applied at $(x, S_D, -d_2)$ and $(x, -S_D, -d_2)$ for the port and starboard hulls where d_2 is defined to be equal to d_1 for fully submerged sections and is $d/2$ for other sections, where d is the transverse projection of the body. The projected area in equation (B.4) is replaced by integrating d. The following contributions result:

$$(B_{22})_{BL+BCD} = -\rho U \int a_{0H} d\, dx + \frac{\rho}{2}\frac{8}{3\pi} \int d\left(C_{DHP}|v_P| + C_{DHS}|v_S|\right) dx$$

$$(B_{24})_{BL+BCD} = -\rho U \int d_2 a_{0H} d\, dx + \frac{\rho}{2}\frac{8}{3\pi} \int d_2 d\left(C_{DHP}|v_P| + C_{DHS}|v_S|\right) dx$$

$$(B_{26})_{BL+BCD} = -\rho U \int x a_{0H} d\, dx + \frac{\rho}{2}\frac{8}{3\pi} \int x d\left(C_{DHP}|v_P| + C_{DHS}|v_S|\right) dx$$

$$(C_{26})_{BL+BCD} = \rho U^2 \int a_{0H} d\, dx$$

$$(F_2)_{BL+BCD} = \rho U \omega A \sin\beta \int a_{0H} d \cos(kS_D \sin\beta) e^{-kd_2+ikx\cos\beta} dx$$

$$-\frac{\rho}{2}\frac{8}{3\pi} \omega A \sin\beta \int d\left(C_{DHP}|v_P|e^{-ikS_D\sin\beta} + C_{DHS}|v_S|e^{ikS_D\sin\beta}\right) e^{-kd_2+ikx\cos\beta} dx$$

where a_{0H} and C_{DHP} and C_{DHS} are the horizontal lift and horizontal cross flow drag coefficients, and the relative velocities for the port and starboard hulls are:

$$v_P = \dot{\xi}_2 + x\dot{\xi}_6 + d_2\dot{\xi}_4 + \omega A \sin\beta e^{-kd_2+ikx\cos\beta-ikS_D\sin\beta}$$

$$v_S = \dot{\xi}_2 + x\dot{\xi}_6 + d_2\dot{\xi}_4 + \omega A \sin\beta e^{-kd_2+ikx\cos\beta+ikS_D\sin\beta}$$

Utilizing equation (B.8) for M_Y, where x_C is defined in Appendix D.

$$(B_{53})_{BL+BCD} = -\rho U \int x a_{0V} d_H dx - \frac{\rho}{2}\frac{8}{3\pi} \int x d_H\left(C_{DVP}|w_P| + C_{DVS}|w_S|\right) dx$$

$$(B_{54})_{BL+BCD} B_{54} = -\frac{\rho}{2}\frac{8}{3\pi} \int S_D x d_H\left(C_{DVP}|w_P| - C_{DVS}|w_S|\right) dx$$

$$(B_{55})_{BL+BCD} = \rho U \int x^2 a_{0V} d_H dx + \frac{\rho}{2}\frac{8}{3\pi} \int x^2 d_H\left(C_{DVP}|w_P| + C_{DVS}|w_S|\right) dx$$

$$(C_{55})_{BL+BCD} = -\rho U^2 \int x a_{0V} d_H dx$$

$$(F_5)_{BL+BCD} = i\rho U \omega A \int x a_{0V} d_H \cos(kS_D \sin\beta) e^{-kd_1+ikx\cos\beta} dx$$

$$+i\omega A \frac{\rho}{2}\frac{8}{3\pi} \int x d_H\left(C_{DVP}|w_P|e^{-ikS_D\sin\beta} + C_{DVS}|w_S|e^{ikS_D\sin\beta}\right) e^{-kd_1+ikx\cos\beta} dx$$

Utilizing equation (B.9) for M_Z,

$$(B_{62})_{BL+BCD} = -\rho U \int x_C a_{0H} d\, dx + \frac{\rho}{2}\frac{8}{3\pi} \int x d\left(C_{DHP}|v_P| + C_{DHS}|v_S|\right) dx$$

$$(B_{64})_{BL+BCD} = -\rho U \int x_C d_2 a_{0H} d\, dx + \frac{\rho}{2}\frac{8}{3\pi} \int x d_2 d\left(C_{DHP}|v_P| + C_{DHS}|v_S|\right) dx$$

$$(B_{66})_{BL+BCD} = -\rho U \int x_C x a_{0H} d\, dx + \frac{\rho}{2}\frac{8}{3\pi} \int x^2 d\left(C_{DHP}|v_P| + C_{DHS}|v_S|\right) dx$$

$$(C_{66})_{BL+BCD} = \rho U^2 \int x_C a_{0H} d\, dx$$

$$(F_6)_{BL+BCD} = \rho U \omega A \sin\beta \int x_C a_{0H} d \cos(kS_D \sin\beta) e^{-kd_2+ikx\cos\beta} dx$$

$$-\frac{\rho}{2}\frac{8}{3\pi} \omega A \sin\beta \int x d\left(C_{DHP}|v_P|e^{-ikS_D\sin\beta} + C_{DHP}|v_S|e^{ikS_D\sin\beta}\right) e^{-kd_2+ikx\cos\beta} dx$$

For lift terms, the moment arm x_C has been used. This is based on the concept that since the transverse projection of the SWATH can be thought of as a wing, the moment associated with lift will not act about the longitudinal center of gravity, but more nearly the quarter chord of the strut. The definition of x_C is given in Appendix D.

48

From equation (B.7) for M_X, with the moment arm for F_Y being $-d_2$ and the one for F_Z being $\pm S_D$, it follows that:

$$(B_{42})_{BL+BCD} = -\rho U \int d_2 a_{0H} d \, dx + \frac{\rho}{2}\frac{8}{3\pi}\int d_2 d\left(C_{DHP}|v_P| + C_{DHS}|v_S|\right) dx$$

$$(B_{43})_{BL+BCD} = \frac{\rho}{2}\frac{8}{3\pi}\int S_D d_H \left(C_{DVP}|w_P| - C_{DVS}|w_S|\right) dx$$

$$(B_{44})_{BL+BCD} = \rho U \int S_D^2 a_{0V} d_H dx + \rho U \int d_2^2 a_{0H} d \, dx$$
$$+ \frac{\rho}{2}\frac{8}{3\pi}\int S_D^2 d_H \left(C_{DVP}|w_P| + C_{DVS}|w_S|\right) dx + \frac{\rho}{2}\frac{8}{3\pi}\int d_2^2 d\left(C_{DHP}|v_P| + C_{DHS}|v_S|\right) dx$$

$$(B_{45})_{BL+BCD} = -\frac{\rho}{2}\frac{8}{3\pi}\int x S_D d_H \left(C_{DVP}|w_P| - C_{DVS}|w_S|\right) dx$$

$$(B_{46})_{BL+BCD} = -\rho U \int x d_2 a_{0H} d \, dx + \frac{\rho}{2}\frac{8}{3\pi}\int x d_2 d\left(C_{DHP}|v_P| + C_{DHS}|v_S|\right) dx$$

$$(C_{46})_{BL+BCD} = \rho U^2 \int d_2 a_{0H} d \, dx$$

$$(F_4)_{BL+BCD} = -\rho U \omega A \int S_D a_{0V} d_H \sin(k S_D \sin\beta) e^{-kd_1 + ikx\cos\beta} dx$$
$$+ \rho U \omega A \sin\beta \int d_2 a_{0H} d \cos(k S_D \sin\beta) e^{-kd_2 + ikx\cos\beta} dx$$
$$- i\frac{\rho}{2}\frac{8}{3\pi}\omega A \int S_D d_H \left(C_{DVP}|w_P| e^{-ikS_D\sin\beta} - C_{DVS}|w_S| e^{ikS_D\sin\beta}\right) e^{-kd_1 + ikx\cos\beta} dx$$
$$- \frac{\rho}{2}\frac{8}{3\pi}\omega A \sin\beta \int d_2 d\left(C_{DHP}|v_P| e^{-ikS_D\sin\beta} + C_{DHS}|v_S| e^{ikS_D\sin\beta}\right) e^{-kd_2 + ikx\cos\beta} dx$$

In order to evaluate these terms, values for the lift and cross flow drag coefficients must be defined. Vertical plane body lift components, horizontal plane body lift components, and cross flow drag coefficients are developed in Appendix C, D, and E, respectively.

49

APPENDIX C - VERTICAL PLANE BODY LIFT CONTRIBUTIONS

In Appendix B, the vertical plane cross flow drag and body lift components for the vertical plane include body lift and cross flow drag coefficients a_{0H}. Experimental results indicated that a consistent definition for a_{0H} led to invalid results. Consequently, semi-empirical expressions developed for submarine derivatives[*] which correspond to the damping terms were utilized as the basis for the body lift terms. The adaptation of these expressions to SWATH configurations is described in reference 6.

$$(B_{33})_{BL} = -\rho L^2 U \left(2.439^{4/3}\sqrt[3]{(k_2 - k_1)m'} - m'\right)$$

$$(B_{35})_{BL} = (B_{53})_{BL} = 0.207\rho L^3 U(k_2 - k_1)m'$$

$$(B_{55})_{BL} = \frac{(B_{35})_{BL}^2}{(B_{33})_{BL}}$$

$$(C_{35})_{BL} = U(B_{33})_{BL}$$

$$(C_{55})_{BL} = -0.278\rho L^3 U^2 (k_2 - k_1)m'$$

where L is the ship length, m' is the displaced volume of the unappended ship divided by ρL^3 and

$$\varepsilon = \sqrt{1 - \left(\frac{d_{H_{max}}}{L}\right)^2}$$

$$\alpha_0 = 2\frac{1-\varepsilon^2}{\varepsilon^3}\left[\frac{1}{2}\ln\frac{1+\varepsilon}{1-\varepsilon} - \varepsilon\right]$$

$$\beta_0 = \frac{1}{\varepsilon^2} - \frac{1-\varepsilon^2}{2\varepsilon^3}\ln\frac{1+\varepsilon}{1-\varepsilon}$$

$$k_1 = \frac{\alpha_0}{2-\alpha_0}$$

$$k_2 = \frac{\beta_0}{2-\beta_0}$$

For the wave exciting forces, a_{0V} should be defined as follows:

$$a_{0V} = \frac{(B_{33})_{BL}}{\rho\int d_H dx}$$

[*] Developed by Elizabeth Dempsey of the David Taylor Model Basin and reported in a report of higher classification.

50

APPENDIX D - TRANSVERSE PLANE BODY LIFT COEFFICIENTS

Transverse Plane Body Lift Coefficients

The portion of a SWATH configuration which is below the waterline can be described as being composed of sections which have both a lower hull and strut, only a submerged lower hull or no lower hull. In the development below, sections which do not have a strut are assumed to be either nose, tail, or parallel sections. In defining lift coefficients, a component approach has been taken. Each sectional component is assumed to have a constant value for the lift coefficients and is taken to be generating a moment about the section's center of pressure.

Nose Section

Utilizing Figure 11 in Hoerner[8], page 19-8, the lift coefficient, a_{0H}, for a plain round fuselage can be estimated as:

$$a_{0H} = 0.009 L_{SECTION} / D_{SECTION}$$

where $L_{SECTION}$ and $D_{SECTION}$ are the length and maximum diameter of the section. The data is for sections with $L_{SECTION}/D_{SECTION}$ ranging from about 6 to 9. From Reference 8, page 19-17, the center of lift, x_c, relative to the nose of the section is:

$$x_C = 0.4 L_{SECTION}$$

Parallel Section

The lift will be neglected since it is theoretically 0.0, and will be small compared to other contributions.

Tail Section

Based on Reference 8, page 19-2:

$$a_{0H} = 0.022$$

From Pitts et al[9], Chart 9, the center of pressure of an ogival nose from the maximum diameter of the tail is approximately,

$$x_C = 0.55 L_{SECTION}$$

Strut Section

If the strut section is taken to be a lifting surface, then, from Whicker-Fehlner[10] for a low aspect ratio control surface in the free stream,

$$a_{0H} = \frac{1.8\pi AR_S}{1.8 + \sqrt{AR_S^2 + 4.}}$$

For the SWATH configuration, AR_S is the aspect ratio of the strut, defined as the average draft divided by the length of the section. The center of pressure is

$$x_C = 0.25 L_{SECTION}$$

from the leading edge of the section.

APPENDIX E - CROSS FLOW DRAG COEFFICIENTS

C_{DVP}, C_{DVS}, C_{DHP}, and C_{DHS} appear in the expressions for the cross flow drag contributions to the coefficients and forces which are presented in Appendix B. Two sets of data are used to evaluate these coefficients. The first set of data is for oscillating plates presented by Bearman and Graham[11] and is given as a function of the Keulegan-Carpenter number, KC. A tabulation of these data is given in Table E.1. The second set is for oscillating cylinders reported by Sarpkaya[12] which is tabulated in Table E.2. Sarpkaya's data is presented as a function of KC, and a frequency parameter, β_{KC}, where

$$KC = \frac{V_{max}T}{d}$$

$$\beta_{KC} = \frac{D^2}{vT}$$

where V_{max} is the amplitude of the velocity, T is the period of oscillation, D is the diameter and v is the kinematic viscosity of the fluid.

The cross flow drag coefficient is assumed to vary along the length of the ship. In applying the data, V_{max} is the amplitude of the relative velocity , v_p, v_s, w_p, or w_s, as appropriate. T is defined using the wave frequency of encounter. For evaluation of C_{DVP} and C_{DVS}, the data for an oscillating cylinder is used with D being the horizontal diameter of the lower hull, d_H. These data are modified by an expression to reflect the influence of the strut on the coefficient[6].

$$C_{DV} = \left(1.0 - \frac{td_V}{d_H}\right)C_D\left(U_m, T, D, v\right)$$

where t is the horizontal thickness of the strut, d_V is the vertical diameter of the lower hull.

C_{DHP} and C_{DHS} are evaluated using either the plate or the cylinder data. For sections where a strut is present, the plate data is used with the local draft used for D. For sections without a strut, the oscillating cylinder is used with D defined as d_V.

Table E.1. Cross flow drag coefficient, C_D as a function of the Keulegan Carpenter number, KC, for flat plates, based on data presented in reference 11.

KC	C_D
2.0	6.75
3.0	5.75
4.0	5.15
5.0	4.75
7.5	3.90
10.0	3.40
15.0	2.95
20.0	2.80

Table E.2. Drag coefficients as a Function of Keulegan Carpenter number and a frequency parameter, based on data presented in reference 12.

	β_{KC}				
KC	497	1107	1985	3123	5260
3.0	1.64	1.40	1.34	1.13	0.85
5.0	1.80	1.65	1.55	1.22	0.95
10.0	2.20	1.95	1.70	1.45	1.00
12.5	2.40	2.05	1.90	1.30	0.90
15.0	2.20	2.00	1.65	1.10	0.85
20.0	2.00	1.70	1.20	0.90	0.75
30.0	1.70	1.40	1.00	0.70	0.60
60.0	1.50	1.05	0.70	0.55	0.50
150.0	1.20	0.90	0.50	0.48	0.42

APPENDIX F - APPENDAGE CONTRIBUTIONS

The contributions of the appendage to the added mass, damping, and restoring coefficients and wave exciting forces are given in this appendix. Summations are taken over all appendages.

Let c_i and b_i be the mean chord and span of the appendage; let Λ_i be the sweep angle of the quarter chord line; let x_{f_i}, y_{f_i}, z_{f_i} be the coordinates of the point on the appendage which is the intersection of the quarter chord and the mean span; let α_i be the cant angle of the appendage relative to the horizon. Assuming an elliptical cross section, the area and added mass can be defined as:

$$A_{f_i} = c_i b_i$$

$$a_{f_i} = \frac{\rho \pi}{4} c_i A_{f_i}$$

C_{D_F} is evaluated using the data given in Appendix E for oscillating plates. While alternate values for the lift curve slope, $C_{L\alpha_i}$, can be specified, the default expression for stabilizers and rudder is:

$$C_{L\alpha_i} = \frac{1.8\pi AR_i}{1.8 + \cos \Lambda_i \sqrt{\dfrac{AR_i^2}{\cos^4 \Lambda_i} + 4.0}} C_{Lc}$$

If $C_{Lc} = 1$, this is the expression developed by Whicker and Fehlner[10] and utilized by Dempsey for submarines.[13] AR_i is the effective aspect ratio of the appendage, which is based on the tip to tip span of a pair of appendages. For SWATHs, unlike submarines, appendages are not used in pairs. However, comparison with experimental results showed that evaluation of $C_{L\alpha_i}$ assuming a pair of fins while evaluating the lift based on the actual stabilizer worked well for SWATHs.[6] C_{Lc} is a modification factor[6] to reflect the effect of downwash from one appendage on another in the same plane - that is, of one stabilizer on another. Therefore, C_{Lc} equals 1.0 except when the appendage is aft of a coplanar appendage. Data presented by Lloyd[14] was corrected for boundary layer effects and tabulated by Cox and Lloyd.[15] C_{Lc} is given in Table F.1.

Table F.1 Ratio of lift on aft fin to lift on forward fin for various fin separations and oscillation frequency-to-speed ratios (from references 14 and 15).

x/b	$\omega b/U$					
	0.00	0.04	0.08	0.12	0.16	0.20
10	0.412	0.544	0.643	0.824	1.076	1.221
15	0.462	0.638	0.846	1.046	1.180	1.109
20	0.529	0.732	1.000	1.151	1.110	0.971
25	0.614	0.816	1.099	1.132	1.101	0.897
30	0.706	0.853	1.118	1.006	0.912	0.853

54

$$(A_{22})_A = \sum a_{f_i} \sin^2 \alpha_i$$

$$(A_{24})_A = -\sum a_{f_i} \sin \alpha_i \left(z_{f_i} \sin \alpha_i + y_{f_i} \cos \alpha_i \right)$$

$$(A_{26})_A = \sum x_{f_i} a_{f_i} \sin^2 \alpha_i$$

$$(A_{33})_A = \sum a_{f_i} \cos^2 \alpha_i$$

$$(A_{35})_A = -\sum x_{f_i} a_{f_i} \cos^2 \alpha_i$$

$$(A_{42})_A = -\sum a_{f_i} \sin \alpha_i \left(z_{f_i} \sin \alpha_i + y_{f_i} \cos \alpha_i \right)$$

$$(A_{44})_A = \sum a_{f_i} \left(z_{f_i} \sin \alpha_i + y_{f_i} \cos \alpha_i \right)^2$$

$$(A_{46})_A = -\sum x_{f_i} a_{f_i} \sin \alpha_i \left(z_{f_i} \sin \alpha_i + y_{f_i} \cos \alpha_i \right)$$

$$(A_{53})_A = -\sum x_{f_i} a_{f_i} \cos^2 \alpha_i$$

$$(A_{55})_A = \sum x_{f_i}^2 a_{f_i} \cos^2 \alpha_i$$

$$(A_{62})_A = \sum x_{f_i} a_{f_i} \sin^2 \alpha_i$$

$$(A_{64})_A = -\sum x_{f_i} a_{f_i} \sin \alpha_i \left(z_{f_i} \sin \alpha_i + y_{f_i} \cos \alpha_i \right)$$

$$(A_{66})_A = \sum x_{f_i}^2 a_{f_i} \sin^2 \alpha_i$$

$$(B_{22})_A = \frac{\rho}{2} U \sum A_{f_i} C_{L\alpha_i} \sin^2 \alpha_i$$

$$(B_{24})_A = -\frac{\rho}{2} U \sum A_{f_i} C_{L\alpha_i} \sin \alpha_i \left(z_{f_i} \sin \alpha_i + y_{f_i} \cos \alpha_i \right)$$

$$(B_{26})_A = \frac{\rho}{2} U \sum x_{f_i} A_{f_i} C_{L\alpha_i} \sin^2 \alpha_i$$

$$(B_{33})_A = \frac{\rho}{2} U \sum A_{f_i} C_{L_{\alpha_i}} \cos^2 \alpha_i + \frac{\rho}{2} \frac{8}{3\pi} \sum A_{f_i} \cos \alpha_i \left(C_{D_{s_i}} \left| w_{s_i} \right| + C_{D_{p_i}} \left| w_{p_i} \right| \right)$$

$$(B_{35})_A = -\frac{\rho}{2} U \sum x_{f_i} A_{f_i} C_{L_{\alpha_i}} \cos^2 \alpha_i - \frac{\rho}{2} \frac{8}{3\pi} \sum x_{f_i} A_{f_i} \cos \alpha_i \left(C_{D_{s_i}} \left| w_{s_i} \right| + C_{D_{p_i}} \left| w_{p_i} \right| \right)$$

$$(B_{42})_A = -\frac{\rho}{2} U \sum A_{f_i} C_{L\alpha_i} \sin \alpha_i \left(z_{f_i} \sin \alpha_i + y_{f_i} \cos \alpha_i \right)$$

$$(B_{44})_A = \frac{\rho}{2} U \sum A_{f_i} C_{L\alpha_i} \left(z_{f_i} \sin \alpha_i + y_{f_i} \cos \alpha_i \right)^2$$

$$(B_{46})_A = -\frac{\rho}{2} U \sum x_{f_i} A_{f_i} C_{L\alpha_i} \sin \alpha_i \left(z_{f_i} \sin \alpha_i + y_{f_i} \cos \alpha_i \right)$$

$$(B_{53})_A = -\frac{\rho}{2} U \sum x_{f_i} A_{f_i} C_{L_{\alpha_i}} \cos^2 \alpha_i - \frac{\rho}{2} \frac{8}{3\pi} \sum x_{f_i} A_{f_i} \cos \alpha_i \left(C_{D_{s_i}} \left| w_{s_i} \right| + C_{D_{p_i}} \left| w_{p_i} \right| \right)$$

$$(B_{55})_A = \frac{\rho}{2} U \sum x_{f_i}^2 A_{f_i} C_{L_{\alpha_i}} \cos^2 \alpha_i + \frac{\rho}{2} \frac{8}{3\pi} \sum x_{f_i}^2 A_{f_i} \cos \alpha_i \left(C_{D_{s_i}} \left| w_{s_i} \right| + C_{D_{p_i}} \left| w_{p_i} \right| \right)$$

$$(B_{62})_A = \frac{\rho}{2} U \sum x_{f_i} A_{f_i} C_{L\alpha_i} \sin^2 \alpha_i$$

$$(B_{64})_A = -\frac{\rho}{2} U \sum x_{f_i} A_{f_i} C_{L\alpha_i} \sin \alpha_i \left(z_{f_i} \sin \alpha_i + y_{f_i} \cos \alpha_i \right)$$

$$(B_{66})_A = \frac{\rho}{2} U \sum x_{f_i}^2 A_{f_i} C_{L\alpha_i} \sin^2 \alpha_i$$

$$(C_{26})_A = \frac{\rho}{2} U^2 \sum x_{f_i} A_{f_i} C_{L_{\alpha_i}} \sin^2 \alpha_i$$

$$(C_{35})_A = \frac{\rho}{2} U^2 \sum A_{f_i} C_{L_{\alpha_i}} \cos^2 \alpha_i$$

$$(C_{55})_A = -\frac{\rho}{2} U^2 \sum x_{f_i} A_{f_i} C_{L_{\alpha_i}} \cos^2 \alpha_i$$

$$(C_{46})_A = -\frac{\rho}{2} U^2 \sum A_{f_i} C_{L\alpha_i} \sin \alpha_i \left(z_{f_i} \sin \alpha_i + y_{f_i} \cos \alpha_i \right)$$

$$(C_{66})_A = \frac{\rho}{2} U^2 \sum x_{f_i}^2 A_{f_i} C_{L_{\alpha_i}} \sin^2 \alpha_i$$

$$(F_2)_A = \frac{\rho}{2} AU\omega \sum A_{f_i} C_{L\alpha_i} \sin \alpha_i \left[\cos \alpha_i \sin\left(ky_{f_i} \sin \beta \right) - \sin \beta \sin \alpha_i \cos\left(ky_{f_i} \sin \beta \right) \right] e^{kz_{f_i} + ikx_{f_i} \cos \beta}$$

$$(F_3)_A = -i \frac{\rho}{2} AU\omega \sum A_{f_i} C_{L\alpha_i} \cos \alpha_i \left[\cos \alpha_i \cos\left(ky_{f_i} \sin \beta \right) + \sin \beta \sin \alpha_i \sin\left(ky_{f_i} \sin \beta \right) \right] e^{kz_{f_i} + ikx_{f_i} \cos \beta}$$

$$- i \frac{\rho}{2} \frac{8}{3\pi} A\omega \sum A_{f_i} \cos \alpha_i \left(C_{D_{s_i}} \left| w_{s_i} \right| e^{ik\left(x_{f_i} \cos \beta + y_{f_i} \sin \beta \right)} + C_{D_{p_i}} \left| w_{p_i} \right| e^{ik\left(x_{f_i} \cos \beta - y_{f_i} \sin \beta \right)} \right) e^{-kz_{f_i}}$$

$$(F_4)_A = -\frac{\rho}{2} AU\omega \sum A_{f_i} C_{L\alpha_i} \left(z_{f_i} \sin \alpha_i + y_{f_i} \cos \alpha_i \right)$$

$$\left[\cos \alpha_i \sin\left(ky_{f_i} \sin \beta \right) - \sin \beta \sin \alpha_i \cos\left(ky_{f_i} \sin \beta \right) \right] e^{kz_{f_i} + ikx_{f_i} \cos \beta}$$

$$(F_5)_A = i \frac{\rho}{2} AU\omega \sum x_{f_i} A_{f_i} C_{L\alpha_i} \cos \alpha_i \left[\cos \alpha_i \cos\left(ky_{f_i} \sin \beta \right) + \sin \beta \sin \alpha_i \sin\left(ky_{f_i} \sin \beta \right) \right] e^{kz_{f_i} + ikx_{f_i} \cos \beta}$$

$$+ i \frac{\rho}{2} \frac{8}{3\pi} A\omega \sum x_{f_i} A_{f_i} \cos \alpha_i \left(C_{D_{s_i}} \left| w_{s_i} \right| e^{ik\left(x_{f_i} \cos \beta + y_{f_i} \sin \beta \right)} + C_{D_{p_i}} \left| w_{p_i} \right| e^{ik\left(x_{f_i} \cos \beta - y_{f_i} \sin \beta \right)} \right) e^{-kz_{f_i}}$$

$$(F_6)_A = \frac{\rho}{2} AU\omega \sum x_{f_i} A_{f_i} C_{L\alpha_i} \sin \alpha_i \left[\cos \alpha_i \sin\left(ky_{f_i} \sin \beta \right) - \sin \beta \sin \alpha_i \cos\left(ky_{f_i} \sin \beta \right) \right] e^{kz_{f_i} + ikx_{f_i} \cos \beta}$$

where

$$w_{P_i} = \dot{\xi}_3 - x_{f_i} \dot{\xi}_5 + y_{f_i} \dot{\xi}_4 + i\omega e^{-kz_{f_i} + ik\left(x_{f_i} \cos \beta - y_{f_i} \sin \beta \right)}$$

$$w_{S_i} = \dot{\xi}_3 - x_{f_i} \dot{\xi}_5 - y_{f_i} \dot{\xi}_4 + i\omega e^{-kz_{f_i} + ik\left(x_{f_i} \cos \beta + y_{f_i} \sin \beta \right)}$$

In the derivation it has been assumed that the appendages have been included in the mass and inertias of the ship and that the origin of the coordinate system is at the appended ship's longitudinal center of gravity. In general, the effect of the fin on the mass matrix will be small. However, in the early design phase the mass properties of a ship is estimated and under some circumstances the appendages may be relatively important. In that case, the mass of the appendages can be estimated by:

$$m_{f_i} = \frac{\rho \pi}{4} A_{f_i} t_i$$

The contributions of the fins to the mass matrix can be estimated by:

$$(m_{22})_A = \sum m_{f_i}$$

$$(m_{24})_A = -\sum z_{f_i} m_{f_i}$$

$$(m_{26})_A = \sum x_{f_i} m_{f_i}$$

$$(m_{33})_A = \sum m_{f_i}$$

$$(m_{35})_A = -\sum x_{f_i} m_{f_i}$$

56

$$(m_{42})_A = -\sum z_{f_i} m_{f_i}$$

$$(m_{44})_A = \sum \left(z_{f_i}^2 + y_{f_i}^2 \right) m_{f_i}$$

$$(m_{46})_A = -\sum x_{f_i} z_{f_i} m_{f_i}$$

$$(m_{53})_A = -\sum x_{f_i} m_{f_i}$$

$$(m_{55})_A = \sum \left(x_{f_i}^2 + z_{f_i}^2 \right) m_{f_i}$$

$$(m_{62})_A = \sum x_{f_i} m_{f_i}$$

$$(m_{64})_A = -\sum x_{f_i} z_{f_i} m_{f_i}$$

$$(m_{66})_A = \sum m_{f_i} \left(x_{f_i}^2 + y_{f_i}^2 \right)$$

APPENDIX G - TOTAL COEFFICIENTS AND FORCES

As noted in the main text of this report, the added mass, damping, and restoring coefficients and wave exciting forces and moments are modeled with potential flow, body lift, body cross flow drag, appendage lift and appendage cross flow drag components. Details of the development of these components are given in Appendices A, B, C, D, E and F. Expressions for the evaluation of the various lift (a_{0H}, a_{0V}, $C_{L\alpha_i}$) and cross flow drag (C_{DH}, C_{DV}, C_{D_F}) coefficients are given in the appendices. Relative vertical velocities are defined by:

$$v_P = \dot{\xi}_2 + x\dot{\xi}_6 + d_2\dot{\xi}_4 + \omega A \sin\beta e^{-kd_2 + ikx\cos\beta - ikS_D\sin\beta}$$

$$v_S = \dot{\xi}_2 + x\dot{\xi}_6 + d_2\dot{\xi}_4 + \omega A \sin\beta e^{-kd_2 + ikx\cos\beta + ikS_D\sin\beta}$$

$$w_P = \dot{\xi}_3 - x\dot{\xi}_5 + S_D\dot{\xi}_4 + i\omega A e^{-kd_1 + ikx\cos\beta - ikS_D\sin\beta}$$

$$w_S = \dot{\xi}_3 - x\dot{\xi}_5 - S_D\dot{\xi}_4 + i\omega A e^{-kd_1 + ikx\cos\beta + ikS_D\sin\beta}$$

$$w_{P_i} = \dot{\xi}_3 - x_{f_i}\dot{\xi}_5 + y_{f_i}\dot{\xi}_4 + i\omega e^{-kz_{f_i} + ik\left(x_{f_i}\cos\beta - y_{f_i}\sin\beta\right)}$$

$$w_{S_i} = \dot{\xi}_3 - x_{f_i}\dot{\xi}_5 - y_{f_i}\dot{\xi}_4 + i\omega e^{-kz_{f_i} + ik\left(x_{f_i}\cos\beta + y_{f_i}\sin\beta\right)}$$

The totals of the components are listed below.

$$A_{22} = \int a_{22}(x)dx + \sum a_{f_i}\sin^2\alpha_i$$

$$A_{24} = \int a_{24}(x)dx - \sum a_{f_i}\sin\alpha_i\left(z_{f_i}\sin\alpha_i + y_{f_i}\cos\alpha_i\right)$$

$$A_{26} = \int x a_{22}(x)dx + \frac{U}{\omega_e^2}\int b_{22}(x)dx + \sum x_{f_i}a_{f_i}\sin^2\alpha_i$$

$$A_{33} = \int a_{33}(x)dx + \sum a_{f_i}\cos^2\alpha_i$$

$$A_{35} = -\int x a_{33}(x)dx - \frac{U}{\omega_e^2}\int b_{33}(x)dx - \sum x_{f_i}a_{f_i}\cos^2\alpha_i$$

$$A_{42} = \int a_{24}(x)dx - \sum a_{f_i}\sin\alpha_i\left(z_{f_i}\sin\alpha_i + y_{f_i}\cos\alpha_i\right)$$

$$A_{44} = \int a_{44}(x)dx + \sum a_{f_i}\left(z_{f_i}\sin\alpha_i + y_{f_i}\cos\alpha_i\right)^2$$

$$A_{46} = \int x a_{24}(x)dx + \frac{U}{\omega_e^2}\int b_{24}(x)dx - \sum x_{f_i}a_{f_i}\sin\alpha_i\left(z_{f_i}\sin\alpha_i + y_{f_i}\cos\alpha_i\right)$$

$$A_{53} = -\int x a_{33}(x)dx + \frac{U}{\omega_e^2}\int b_{33}(x)dx - \sum x_{f_i}a_{f_i}\cos^2\alpha_i$$

$$A_{55} = \int x^2 a_{33}(x)dx + \frac{U^2}{\omega_e^2}\int a_{33}(x)dx + \sum x_{f_i}^2 a_{f_i}\cos^2\alpha_i$$

$$A_{62} = \int x a_{22}(x)dx - \frac{U}{\omega_e^2}\int b_{22}(x)dx + \sum x_{f_i}a_{f_i}\sin^2\alpha_i$$

$$A_{64} = \int x a_{24}(x)dx - \frac{U}{\omega_e^2}\int b_{24}(x)dx - \sum x_{f_i}a_{f_i}\sin\alpha_i\left(z_{f_i}\sin\alpha_i + y_{f_i}\cos\alpha_i\right)$$

$$A_{66} = \int x^2 a_{22}dx + \frac{U^2}{\omega_e^2}\int a_{22}(x)dx + \sum x_{f_i}^2 a_{f_i}\sin^2\alpha_i$$

$$B_{22} = \int b_{22}(x)dx + \frac{\rho}{2}U\sum A_{f_i}C_{L\alpha_i}\sin^2\alpha_i$$
$$-\rho U\int a_{0H}d\,dx + \frac{\rho}{2}\frac{8}{3\pi}\int d\left(C_{DHP}|v_P| + C_{DHS}|v_S|\right)dx$$

$$B_{24} = \int b_{24}(x)dx - \frac{\rho}{2}U\sum A_{f_i}C_{L\alpha_i}\sin\alpha_i\left(z_{f_i}\sin\alpha_i + y_{f_i}\cos\alpha_i\right)$$
$$-\rho U\int d_2 a_{0H}d\,dx + \frac{\rho}{2}\frac{8}{3\pi}\int d_2 d\left(C_{DHP}|v_P| + C_{DHS}|v_S|\right)dx$$

$$B_{26} = \int xb_{22}(x)dx - U\int a_{22}(x)dx + \frac{\rho}{2}U\sum x_{f_i}A_{f_i}C_{L\alpha_i}\sin^2\alpha_i$$
$$-\rho U\int xa_{0H}d\,dx + \frac{\rho}{2}\frac{8}{3\pi}\int xd\left(C_{DHP}|v_P| + C_{DHS}|v_S|\right)dx$$

$$B_{33} = \int b_{33}(x)dx + \frac{\rho}{2}U\sum A_{f_i}C_{L_{\alpha_i}}\cos^2\alpha_i + \frac{\rho}{2}\frac{8}{3\pi}\sum A_{f_i}\cos\alpha_i\left(C_{D_{s_i}}\left|w_{s_i}\right| + C_{D_{p_i}}\left|w_{p_i}\right|\right)$$
$$-\rho L^2 U\left(2.439^{4/3}\sqrt[3]{(k_2 - k_1)m'} - m'\right) + \frac{\rho}{2}\frac{8}{3\pi}\int d_H\left(C_{DVP}|w_P| + C_{DVS}|w_S|\right)dx$$

$$B_{34} = \frac{\rho}{2}\frac{8}{3\pi}\int S_D d_H\left(C_{DVP}|w_P| - C_{DVS}|w_S|\right)dx$$

$$B_{35} = -\int xb_{33}(x)dx + U\int a_{33}(x)dx$$
$$-\frac{\rho}{2}U\sum x_{f_i}A_{f_i}C_{L_{\alpha_i}}\cos^2\alpha_i - \frac{\rho}{2}\frac{8}{3\pi}\sum x_{f_i}A_{f_i}\cos\alpha_i\left(C_{D_{s_i}}\left|w_{s_i}\right| + C_{D_{p_i}}\left|w_{p_i}\right|\right)$$
$$+0.207\rho L^3 U(k_2 - k_1)m' - \frac{\rho}{2}\frac{8}{3\pi}\int xd_H\left(C_{DVP}|w_P| + C_{DVS}|w_S|\right)dx$$

$$B_{42} = \int b_{24}(x)dx - \frac{\rho}{2}U\sum A_{f_i}C_{L\alpha_i}\sin\alpha_i\left(z_{f_i}\sin\alpha_i + y_{f_i}\cos\alpha_i\right)$$
$$-\rho U\int d_2 a_{0H}d\,dx + \frac{\rho}{2}\frac{8}{3\pi}\int d_2 d\left(C_{DHP}|v_P| + C_{DHS}|v_S|\right)dx$$

$$B_{43} = \frac{\rho}{2}\frac{8}{3\pi}\int S_D d_H\left(C_{DVP}|w_P| - C_{DVS}|w_S|\right)dx$$

$$B_{44} = \int b_{44}(x)dx + \frac{\rho}{2}U\sum A_{f_i}C_{L\alpha_i}\left(z_{f_i}\sin\alpha_i + y_{f_i}\cos\alpha_i\right)^2$$
$$+\rho U\int S_D^2 a_{0V}d_H dx + \rho U\int d_2^2 a_{0H}d\,dx$$
$$+\frac{\rho}{2}\frac{8}{3\pi}\int S_D^2 d_H\left(C_{DVP}|w_P| + C_{DVS}|w_S|\right)dx + \frac{\rho}{2}\frac{8}{3\pi}\int d_2^2 d\left(C_{DHP}|v_P| + C_{DHS}|v_S|\right)dx$$

$$B_{45} = -\frac{\rho}{2}\frac{8}{3\pi}\int xS_D d_H\left(C_{DVP}|w_P| - C_{DVS}|w_S|\right)dx$$

$$B_{46} = \int xb_{24}(x)dx - U\int a_{24}(x)dx - \frac{\rho}{2}U\sum x_{f_i}A_{f_i}C_{L\alpha_i}\sin\alpha_i\left(z_{f_i}\sin\alpha_i + y_{f_i}\cos\alpha_i\right)$$
$$-\rho U\int xd_2 a_{0H}d\,dx + \frac{\rho}{2}\frac{8}{3\pi}\int xd_2 d\left(C_{DHP}|v_P| + C_{DHS}|v_S|\right)dx$$

$$B_{53} = -\int xb_{33}(x)dx - U\int a_{33}(x)dx$$
$$-\frac{\rho}{2}U\sum x_{f_i}A_{f_i}C_{L_{\alpha_i}}\cos^2\alpha_i - \frac{\rho}{2}\frac{8}{3\pi}\sum x_{f_i}A_{f_i}\cos\alpha_i\left(C_{D_{s_i}}\left|w_{s_i}\right| + C_{D_{p_i}}\left|w_{p_i}\right|\right)$$
$$+0.207\rho L^3 U(k_2 - k_1)m' - \frac{\rho}{2}\frac{8}{3\pi}\int xd_H\left(C_{DVP}|w_P| + C_{DVS}|w_S|\right)dx$$

$$B_{54} = -\frac{\rho}{2}\frac{8}{3\pi}\int S_D xd_H\left(C_{DVP}|w_P| - C_{DVS}|w_S|\right)dx$$

$$B_{55} = \int x^2 b_{33}(x)dx + \frac{U^2}{\omega_e^2}\int b_{33}(x)dx$$

$$+ \frac{\rho}{2}U\sum x_{f_i}^2 A_{f_i} C_{L_{\alpha_i}} \cos^2\alpha_i + \frac{\rho}{2}\frac{8}{3\pi}\sum x_{f_i}^2 A_{f_i}\cos\alpha_i\left(C_{D_{s_i}}|w_{s_i}| + C_{D_{p_i}}|w_{p_i}|\right)$$

$$-\rho L^4 U \frac{(0.207(k_2 - k_1)m')^2}{2.439^{4/3}\sqrt[3]{(k_2 - k_1)m'} - m'} + \frac{\rho}{2}\frac{8}{3\pi}\int x^2 d_H\left(C_{DVP}|w_P| + C_{DVS}|w_S|\right)dx$$

$$B_{62} = \int x b_{22}(x)dx + U\int a_{22}(x)dx + \frac{\rho}{2}U\sum x_{f_i} A_{f_i} C_{L\alpha_i}\sin^2\alpha_i$$

$$-\rho U\int x_C a_{0H} ddx + \frac{\rho}{2}\frac{8}{3\pi}\int x d\left(C_{DHP}|v_P| + C_{DHS}|v_S|\right)dx$$

$$B_{64} = \int x b_{24}(x)dx + U\int a_{24}(x)dx - \frac{\rho}{2}U\sum x_{f_i} A_{f_i} C_{L\alpha_i}\sin\alpha_i\left(z_{f_i}\sin\alpha_i + y_{f_i}\cos\alpha_i\right)$$

$$-\rho U\int x_C d_2 a_{0H} ddx + \frac{\rho}{2}\frac{8}{3\pi}\int x d_2 d\left(C_{DHP}|v_P| + C_{DHS}|v_S|\right)dx$$

$$B_{66} = \int x^2 b_{22}dx + \frac{U^2}{\omega_e^2}\int b_{22}(x)dx + \frac{\rho}{2}U\sum x_{f_i}^2 A_{f_i} C_{L\alpha_i}\sin^2\alpha_i$$

$$-\rho U\int x_C x a_{0H} ddx + \frac{\rho}{2}\frac{8}{3\pi}\int x^2 d\left(C_{DHP}|v_P| + C_{DHS}|v_S|\right)dx$$

$$C_{26} = \rho U^2\int a_{0H} ddx + \frac{\rho}{2}U^2\sum x_{f_i} A_{f_i} C_{L_{\alpha_i}}\sin^2\alpha_i$$

$$C_{33} = \rho g\int t dx$$

$$C_{35} = \rho g\int x t dx + \frac{\rho}{2}U^2\sum A_{f_i} C_{L_{\alpha_i}}\cos^2\alpha_i - \rho L^2 U^2\left(2.439^{4/3}\sqrt[3]{(k_2 - k_1)m'} - m'\right)$$

$$C_{44} = \rho g\int y^2 t dx - Mg\overline{BG}$$

$$C_{46} = -\frac{\rho}{2}U^2\sum A_{f_i} C_{L\alpha_i}\sin\alpha_i\left(z_{f_i}\sin\alpha_i + y_{f_i}\cos\alpha_i\right) + \rho U^2\int d_2 a_{0H} ddx$$

$$C_{53} = \rho g\int x t dx$$

$$C_{55} = \rho g\int x^2 t dx - Mg\overline{BG} - \frac{\rho}{2}U^2\sum x_{f_i} A_{f_i} C_{L_{\alpha_i}}\cos^2\alpha_i - 0.278\rho L^3 U^2(k_2 - k_1)m'$$

$$C_{66} = \frac{\rho}{2}U^2\sum x_{f_i}^2 A_{f_i} C_{L_{\alpha_i}}\sin^2\alpha_i + \rho U^2\int x_C a_{0H} ddx$$

With symmetry of the ship about the ship's centerline assumed, the contributions to the wave exciting forces due to potential flow are:

$$F_2 = -2\rho g A\int dx e^{ikx\cos\beta}\int_{C(x)}\left\{in_2\sin(ky\sin\beta) + \frac{k}{\omega}\left[n_2\sin\beta\cos(ky\sin\beta) + n_3\sin(ky\sin\beta)\right]\phi_2\right\}e^{kz}dl$$

$$+ \frac{\rho}{2}AU\omega\sum A_{f_i} C_{L\alpha_i}\sin\alpha_i\left[\cos\alpha_i\sin\left(ky_{f_i}\sin\beta\right) - \sin\beta\sin\alpha_i\cos\left(ky_{f_i}\sin\beta\right)\right]e^{kz_{f_i} + ikx_{f_i}\cos\beta}$$

$$+ \rho U\omega A\sin\beta\int a_{0H}d\cos(kS_D\sin\beta)e^{-kd_2 + ikx\cos\beta}dx$$

$$- \frac{\rho}{2}\frac{8}{3\pi}\omega A\sin\beta\int de^{-kd_2 + ikx\cos\beta}\left(C_{DHP}|v_P|e^{-ikS_D\sin\beta} + C_{DHS}|v_S|e^{ikS_D\sin\beta}\right)dx$$

60

$$F_3 = 2\rho g A \int dx e^{ikx\cos\beta} \int\limits_{C(x)} \left\{ n_3\cos(ky\sin\beta) + i\frac{k}{\omega}\left[n_2\sin\beta\sin(ky\sin\beta) - n_3\cos(ky\sin\beta)\right]\phi_3 \right\} e^{kz} dl$$

$$-i\frac{\rho}{2}AU\omega\sum A_{f_i}C_{L\alpha_i}\cos\alpha_i\left[\cos\alpha_i\cos\left(ky_{f_i}\sin\beta\right) + \sin\beta\sin\alpha_i\sin\left(ky_{f_i}\sin\beta\right)\right]e^{kz_{f_i}+ikx_{f_i}\cos\beta}$$

$$-i\frac{\rho}{2}\frac{8}{3\pi}A\omega\sum A_{f_i}\cos\alpha_i\left(C_{D_{s_i}}\left|w_{s_i}\right|e^{ik\left(x_{f_i}\cos\beta+y_{f_i}\sin\beta\right)} + C_{D_{p_i}}\left|w_{p_i}\right|e^{ik\left(x_{f_i}\cos\beta-y_{f_i}\sin\beta\right)}\right)e^{-kz_{f_i}}$$

$$-i\rho U\omega A\int a_{0V}d_H\cos(kS_D\sin\beta)e^{-kd_1+ikx\cos\beta}dx$$

$$-i\omega A\frac{\rho}{2}\frac{8}{3\pi}\int d_H\left(C_{DVP}\left|w_P\right|e^{-ikS_D\sin\beta} + C_{DVS}\left|w_S\right|e^{ikS_D\sin\beta}\right)e^{-kd_1+ikx\cos\beta}dx$$

$$F_4 = -2\rho g A\int dx e^{ikx\cos\beta}$$

$$\int\limits_{C(x)} \left\{ i\left[yn_3 - zn_2\right]\sin(ky\sin\beta) + \frac{k}{\omega}\left[n_2\sin\beta\cos(ky\sin\beta) + n_3\sin(ky\sin\beta)\right]\phi_4 \right\} e^{kz} dl$$

$$-\frac{\rho}{2}AU\omega\sum A_{f_i}C_{L\alpha_i}\left(z_{f_i}\sin\alpha_i + y_{f_i}\cos\alpha_i\right)$$

$$\left[\cos\alpha_i\sin\left(ky_{f_i}\sin\beta\right) - \sin\beta\sin\alpha_i\cos\left(ky_{f_i}\sin\beta\right)\right]e^{kz_{f_i}+ikx_{f_i}\cos\beta}$$

$$-\rho U\omega A\int S_D a_{0V}d_H\sin(kS_D\sin\beta)e^{-kd_1+ikx\cos\beta}dx$$

$$+\rho U\omega A\sin\beta\int d_2 a_{0H}d\cos(kS_D\sin\beta)e^{-kd_2+ikx\cos\beta}dx$$

$$-i\frac{\rho}{2}\frac{8}{3\pi}\omega A\int S_D d_H\left(C_{DVP}\left|w_P\right|e^{-ikS_D\sin\beta} - C_{DVS}\left|w_S\right|e^{ikS_D\sin\beta}\right)e^{-kd_1+ikx\cos\beta}dx$$

$$-\frac{\rho}{2}\frac{8}{3\pi}\omega A\sin\beta\int d_2 d\left(C_{DHP}\left|v_P\right|e^{-ikS_D\sin\beta} + C_{DHS}\left|v_S\right|e^{ikS_D\sin\beta}\right)e^{-kd_2+ikx\cos\beta}dx$$

$$F_5 = -2\rho g A\int dx e^{ikx\cos\beta}$$

$$\int\limits_{C(x)} \left\{ xn_3\cos(ky\sin\beta) + i\frac{k}{\omega}\left[x - \frac{U}{i\omega_e}\right]\left[n_2\sin\beta\sin(ky\sin\beta) - n_3\cos(ky\sin\beta)\right]\phi_3 \right\} e^{kz} dl$$

$$+i\frac{\rho}{2}AU\omega\sum x_{f_i}A_{f_i}C_{L\alpha_i}\cos\alpha_i\left[\cos\alpha_i\cos\left(ky_{f_i}\sin\beta\right) + \sin\beta\sin\alpha_i\sin\left(ky_{f_i}\sin\beta\right)\right]e^{kz_{f_i}+ikx_{f_i}\cos\beta}$$

$$+i\frac{\rho}{2}\frac{8}{3\pi}A\omega\sum x_{f_i}A_{f_i}\cos\alpha_i$$

$$\left(C_{D_{s_i}}\left|w_{s_i}\right|e^{ik\left(x_{f_i}\cos\beta+y_{f_i}\sin\beta\right)} + C_{D_{p_i}}\left|w_{p_i}\right|e^{ik\left(x_{f_i}\cos\beta-y_{f_i}\sin\beta\right)}\right)e^{-kz_{f_i}}$$

$$+i\rho U\omega A\int x a_{0V}d_H\cos(kS_D\sin\beta)e^{-kd_1+ikx\cos\beta}dx$$

$$+i\omega A\frac{\rho}{2}\frac{8}{3\pi}\int x d_H\left(C_{DVP}\left|w_P\right|e^{-ikS_D\sin\beta} + C_{DVS}\left|w_S\right|e^{ikS_D\sin\beta}\right)e^{-kd_1+ikx\cos\beta}dx$$

$$F_6 = -2\rho gA \int dx e^{ikx\cos\beta}$$

$$\int_{C(x)} \left\{ ixn_2 \sin(ky\sin\beta) + \frac{k}{\omega}\left[x - \frac{U}{i\omega_e}\right]\left[n_2 \sin\beta\cos(ky\sin\beta) + n_3 \sin(ky\sin\beta)\right]\phi_2 \right\} e^{kz} dl$$

$$+ \frac{\rho}{2}AU\omega \sum x_{f_i} A_{f_i} C_{L\alpha_i} \sin\alpha_i \left[\cos\alpha_i \sin\left(ky_{f_i}\sin\beta\right) - \sin\beta\sin\alpha_i \cos\left(ky_{f_i}\sin\beta\right)\right] e^{kz_{f_i} + ikx_{f_i}\cos\beta}$$

$$+ \rho U\omega A \sin\beta \int x_C a_{0H} d\cos(kS_D \sin\beta) e^{-kd_2 + ikx\cos\beta} dx$$

$$- \frac{\rho}{2}\frac{8}{3\pi}\omega A \sin\beta \int x d\left(C_{DHP}|v_P|e^{-ikS_D\sin\beta} + C_{DHP}|v_S|e^{ikS_D\sin\beta}\right) e^{-kd_2 + ikx\cos\beta} dx$$

$$F_1 = -2i\rho gAk\cos\beta \iiint e^{kz + ikx\cos\beta} \cos(ky\sin\beta) dz dy dx$$

$$F_{51} = 2i\rho gAk\cos\beta \iiint z e^{kz + ikx\cos\beta} \cos(ky\sin\beta) dz dy dx$$

REFERENCES

1. McCreight, K. K., "Assessing the Seaworthiness of SWATH Ships," Transactions of the Society of Naval Architects and Marine Engineers, Vol. 95, pp. 189-214.

2. Salvesen, N., Tuck, E.O., and Faltinsen, O., "Ship Motions and Sea Loads," Transactions of the Society of Naval Architects and Marine Engineers, Vol. 78, 1970.

3. Lee, C.M., "Theoretical Prediction of Motion of Small-Waterplane Area, Twin-Hull (SWATH) Ships in Waves," DTNSRDC Report SPD-76-0046, December 1976.

4. Incompressible Aerodynamics, edited by B. Thwaites, Oxford University Press, 1960, pp 405-421.

5. Hong, Y.S., "Improvements in the Prediction of Heave and Pitch Motions for SWATH Ships," DTNSRDC Report SPD-0928-02, April 1980.

6. McCreight, K.K. and Stahl, R., "Vertical Plane Motions of SWATH Ships in Regular Waves," DTNSRDC Report SPD-1076-01, June 1983.

7. Frank, W., "Oscillation of Cylinders in or Below the Free Surface of Deep Fluids," Hydromechanics Laboratory Research and Development Report 2375, October 1967.

8. Hoerner, S. F., and H. V. Borst, Fluid-Dynamic Lift, published by Liselotte A. Hoerner, 1985.

9. Pitts, William C., Nielsen, Jack N., and Kaattari, George E., "Lift and Center of Pressure of Wing-Body-Tail Combinations at Subsonic, Transonic, and Supersonic Speeds," NACA Report 1307.

10. Whicker, L.F. and Fehlner, L. F. , "Free-Stream Characteristics of a Family of Low-Aspect-Ratio, All-Movable Control Surfaces for Application to Ship Design," DTMB Report 933, Revised Edition, December 1958.

11. Bearman, P.W. and Graham, J.M.R. , "Hydrodynamic Forces on Cylindrical Bodies in Oscillatory Flow," Second International Conference on Behavior of Off-Shore Structures, Paper 24, August 1979.

12. Sarpkaya, T., "In-Line and Transverse Forces on Cylinders in Oscillatory Flow at High Reynolds Numbers," Journal of Ship Research, Vol. 21, No. 4, December 1977.

13. Dempsey, Elizabeth M., "Static Stability Characteristics of a Systematic Series of Stern Control Surfaces on a Body of Revolution," DTNSRDC Report 77-0085, August 1977.

14. Lloyd, A.R.J.M., "Roll Stabiliser Fins: Interference at Non-Zero Frequencies, Transactions, Royal Institute of Naval Architects, Vol. 1127, 1975.

15. Cox, G.G. and Lloyd, A.R., "Hydrodynamic Design Basis for Navy Ship Roll Motion Stabilization," Transactions, SNAME, Vol. 85, 1977.

16. Kallio, J. A., "Seaworthiness Characteristics of a 2900 Ton Small Waterplane Area Twin Hull (SWATH)", DTNSRDC/SPD-620-03, September 1976.